Edge Localised Modes: ELMs

J W Connor
Culham Science Centre
Abingdon, UK

ITER School
Aix-en-Provence, France
July 2007

Acknowledgements: A Kirk, H Wilson

Questions

ELMs

- **What are they?**
- **Why do they matter?**
- **What causes them?**
- **Can we control them?**

History: L and H-modes

- **Adding external heating power to Ohmically heated tokamaks produced L-mode discharges with degraded confinement**

- **Serendipitously, ASDEX showed a sudden transition to the higher confinement H-mode above a certain threshold power, $P_{L\text{-}H}$**
  - since found in all tokamaks with $P > P_{L\text{-}H}$

- **The H-mode has steep edge gradients associated with an edge transport barrier giving improved confinement**

Evolution of Edge Density Profile (ASDEX)

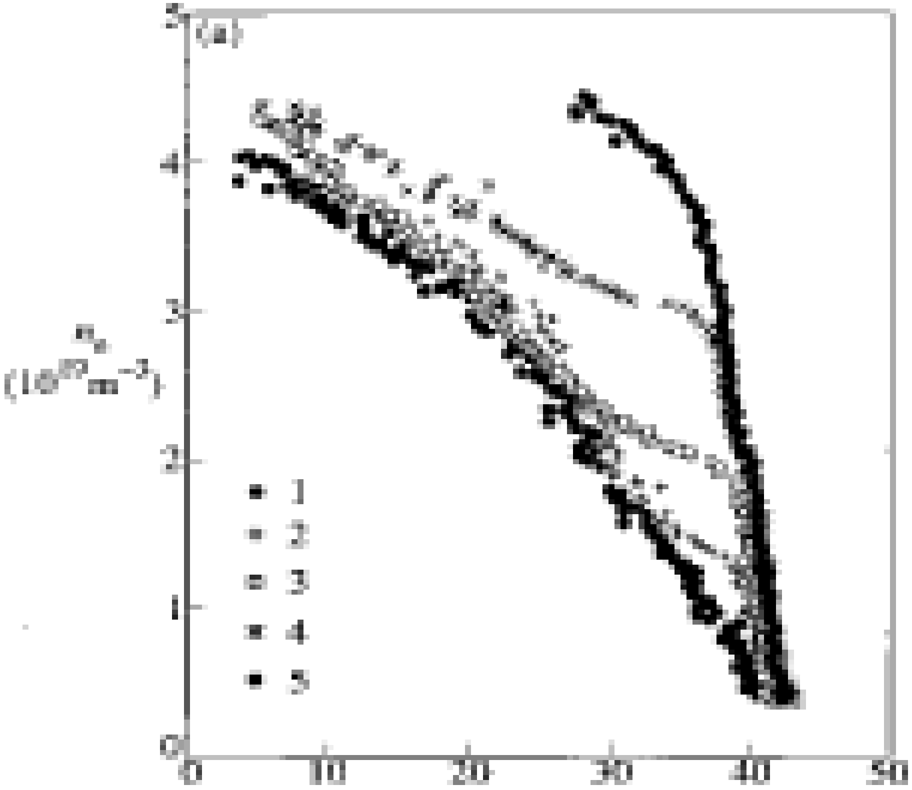

Edge Pedestal (JET)

n_e, T_e, T_i

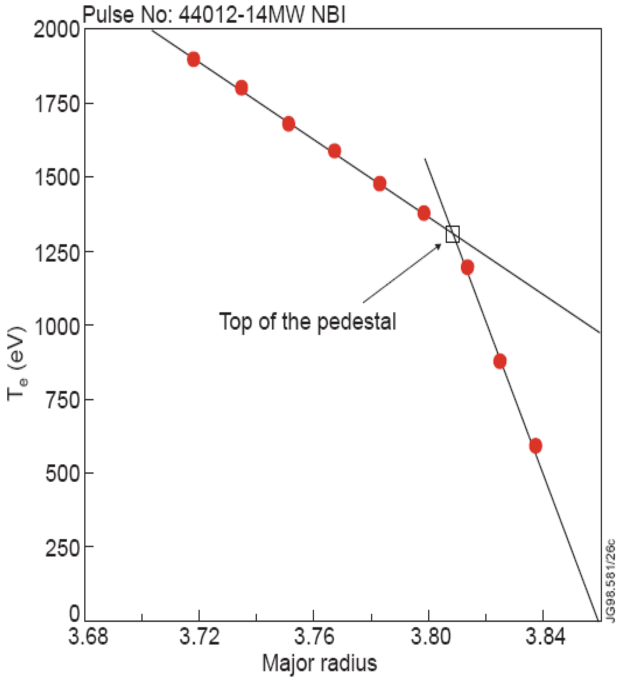

Fig. 4.1. Electron temperature profile measured with the ECE heterodyne radiometer. This profile was taken during the stationary phase of an ELMy H-mode (pulse #44012, 14 MW NBI), in-between two Type I ELMs. The closed circles indicate the experimental points and the open square the extrapolated position of the edge pedestal. (From Ref. [11].)

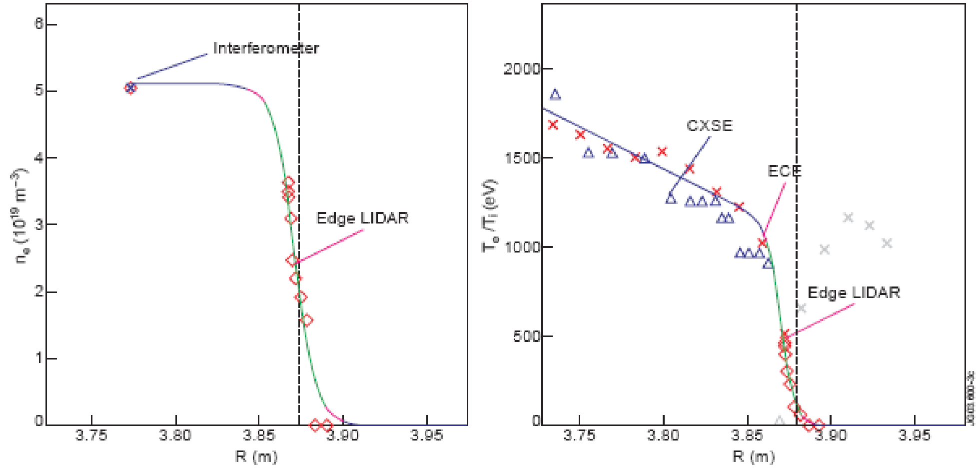

Fig. 4.3. Radial edge profiles of electron density and electron and ion temperature taken from interferometry, edge LIDAR, CXSE and ECE. Fits of hyperbolic tangent functions to the electron density and temperature data are shown as a solid line. (From Ref. [116].)

Schematic Profile

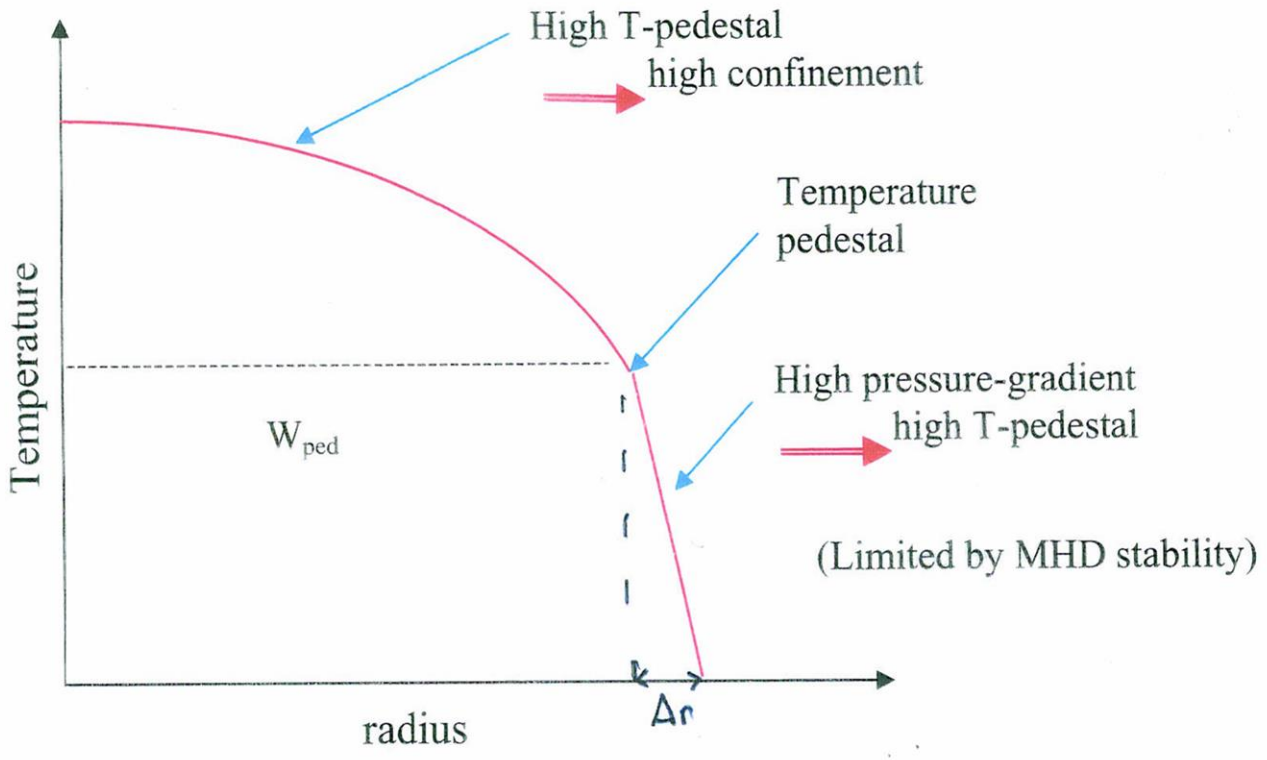

ITER Baseline Scenario - Plasma

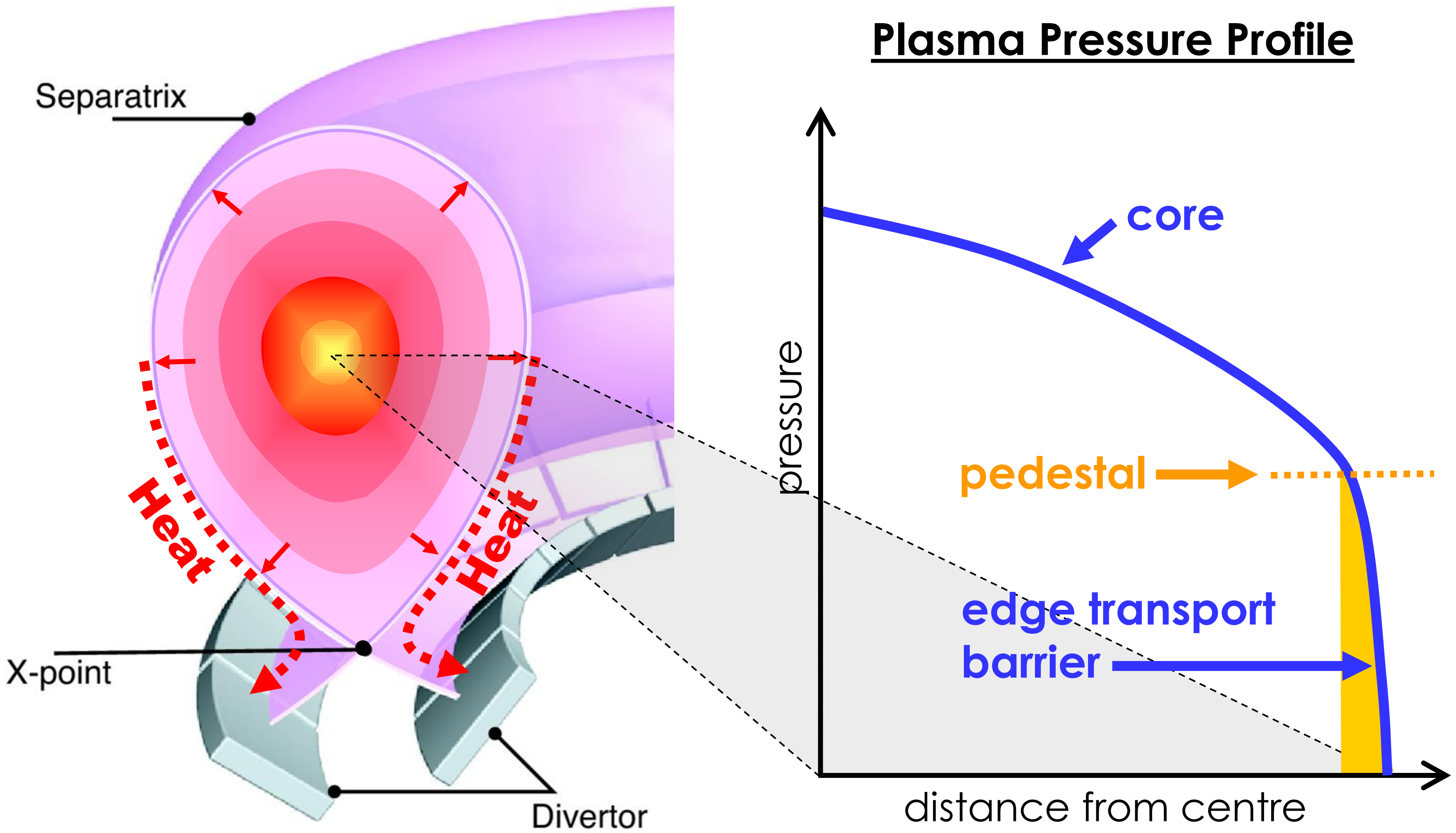

ELMs

- However this was accompanied by instabilities at the plasma edge: ELMs
- Short bursts ejecting edge plasma
- Remove impurities and help control plasma density
- BUT can trigger large MHD events
- AND cause unacceptable erosion on divertors

ELM Heat Losses

- rapidly eject heat and particles

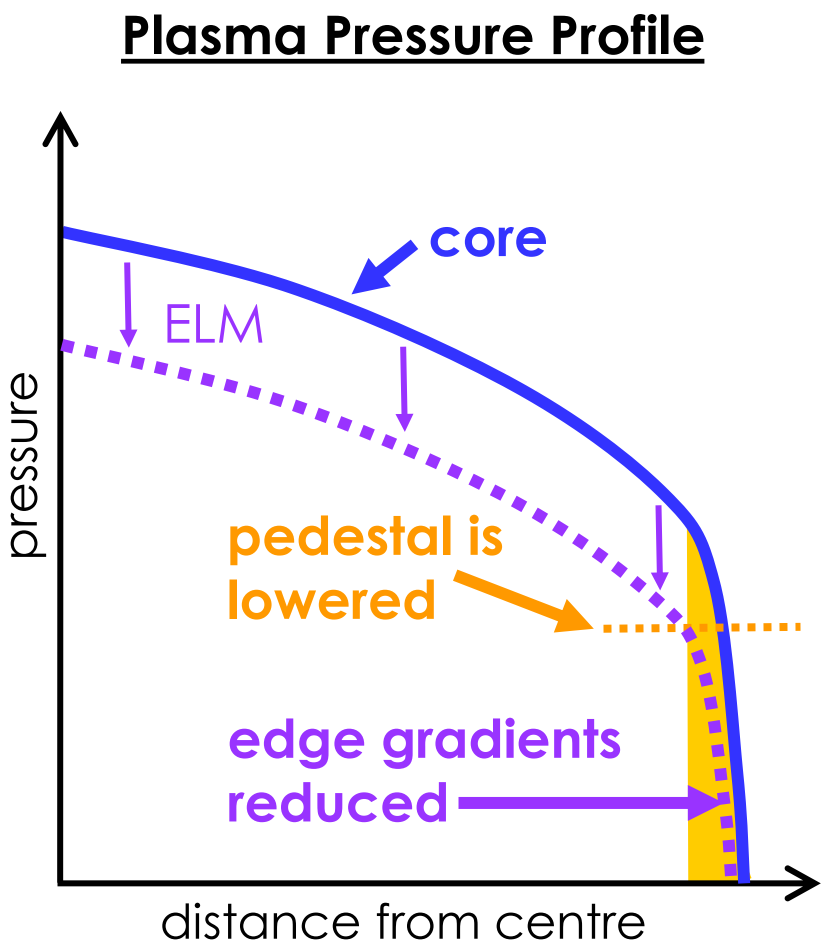

- Steep gradients drive instability
  - Pressure helps overcome magnetic containment
  - Peels off edge of plasma & drops gradients
- Energy dumped outside plasma:
  - carried along field lines to divertor

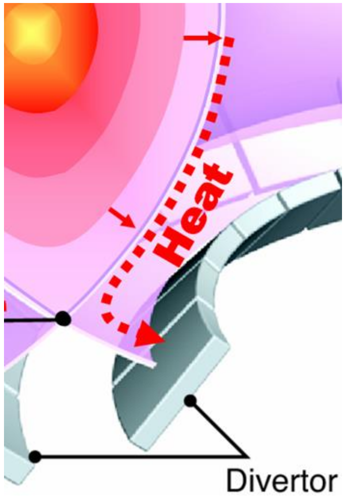

ELMs Ablate the Divertor Tiles

- Ablation process rises sharply above a threshold in energy
  - note for ITER: energy goes as $(\text{size})^3$ while tile area $\propto(\text{size})^2$

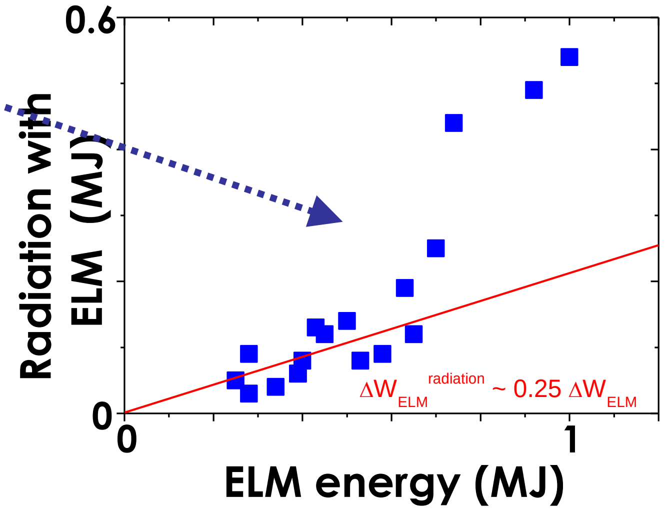

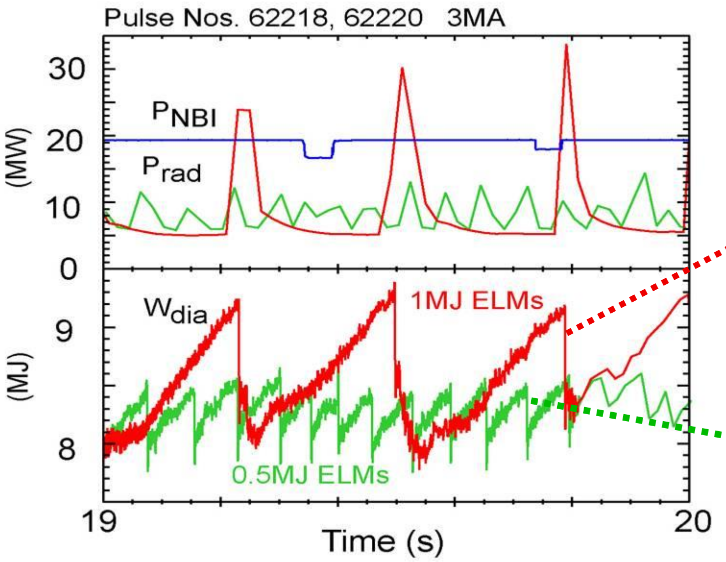

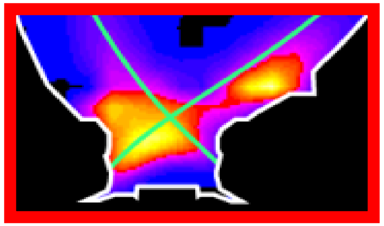

1MJ ELMs lead to strong ablation and so high radiation

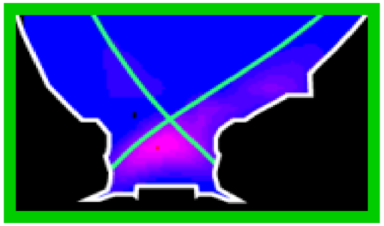

0.5MJ ELMs lead to minimal ablation and so low radiation

Outline of ELM Characteristics

ELM Characteristics

- D_α (H_α) trace $\Longrightarrow$ periodic enhanced plasma wall interaction
- Different types: Type I, Type III etc (later)
- Magnetic signals on Mirnov coils as 'precursors'
  $\Longrightarrow$ MHD instability?
- Periodic loss of plasma in edge pedestal
  $\Longrightarrow$ fluctuation-enhanced losses
- Visible camera pictures $\Longrightarrow$ 'filaments'
- Fast electrons at divertor $\Longrightarrow$ magnetic reconnection?

D_α Traces (JET): Types I & III

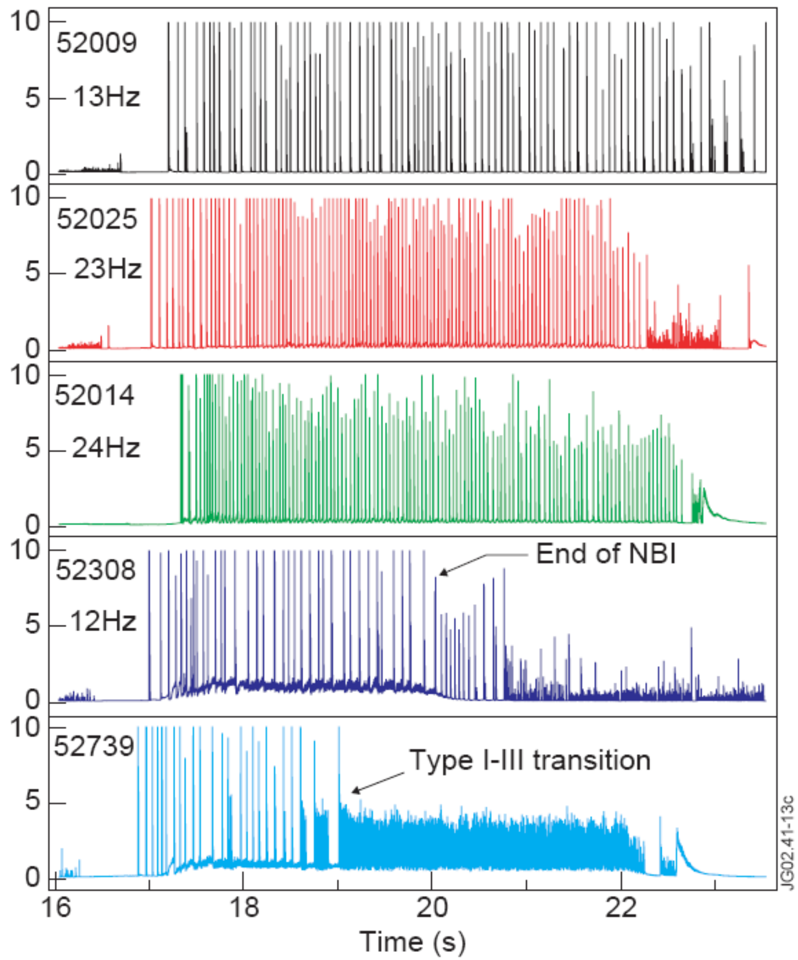

Fig. 4.7. Time traces of the D_α emission from the outer divertor region for five discharges in a density scan at 2.5 MA/2.7 T, δ=0.47. The pulses are in order of increasing gas fuelling with the lowest fuelling in the uppermost box. All discharges are NBI heated with a high power flat of 13.5 - 15 MW beginning at ≈17 seconds and extending to ≈20 seconds for #52308 and beyond 22 seconds for the rest. The discharge number is given for each box along with the mean Type I ELM frequency during the main Type I or Type I-II ELMy H-mode phase. (From Ref. [13].)

Magnetic Signals

MHD Characteristics of ELMs on ASDEX Upgrade

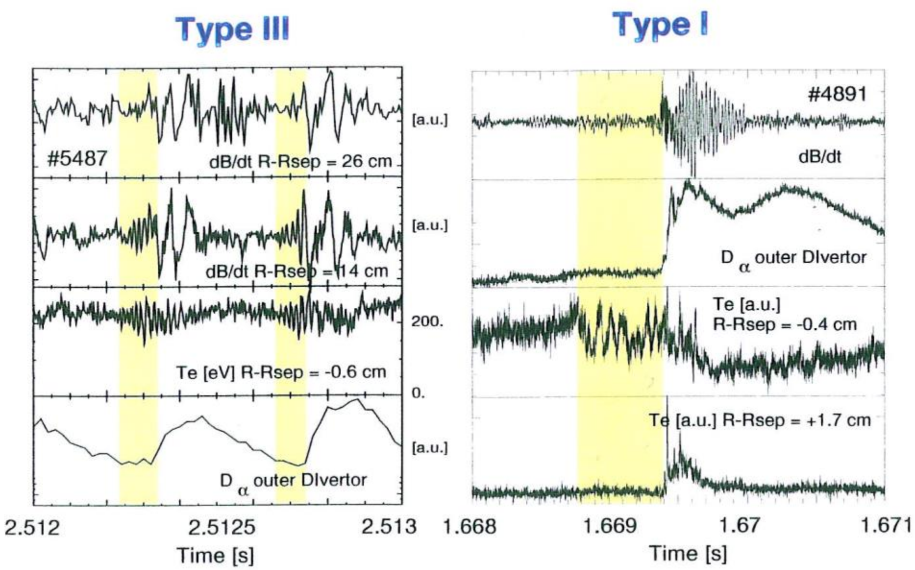

- Type III ELM exhibits magnetic precursor
  - υ = 75 kHz, m ≈ 10, very edge localized (< 4 cm)
- Type I ELM has no (detectable) magnetic precursor for co-injection
- Type I ELM precursor on ECE for co.
  - either electrostatic or very high m (> 20)
- Transport during type I ELM turbulent

ELM Effect on Stored Energy (JET)

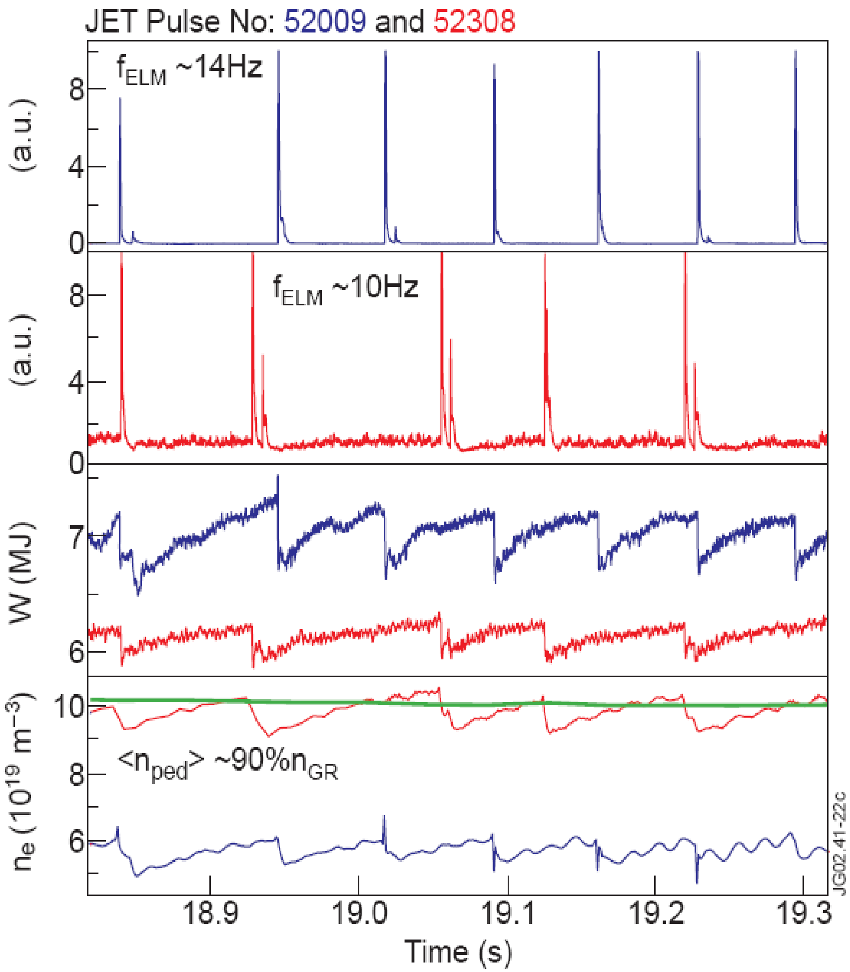

Fig. 4.8. Comparison of the D_α emission from the outer divertor region for two of the pulses in Fig. 4.7 (box 1 and 2). The respective total plasma stored energies (box 3, taken directly from the diamagnetic measurement) and line average densities (box 4) are also shown. The dashed line in box 4 represents the Greenwald density limit.

Effect of ELM Frequency on Confinement

CONFINEMENT AND LOSSES

Degradation of τ_E

- $\tau_E^{ELMyH} \simeq \eta \tau_E^{ELM-freeH} \quad : \quad \eta \simeq 0.85$

  Physics basis (Zohm)

$$\eta = 1 - \left[1 - \left(\frac{r_{ELM}}{a}\right)^2\right] \frac{f_{ELM}\delta W}{P}$$

- H-factor

  $H \equiv \dfrac{\tau^H}{\tau^L}$

  JT-60U

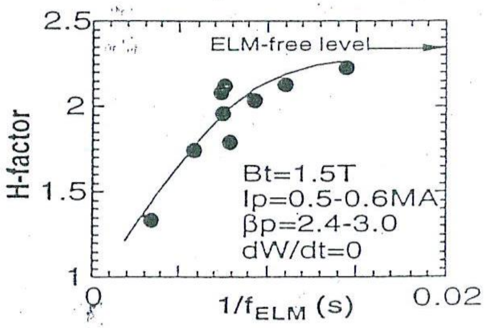

Energy Confinement v ELM Frequency

Energy confinement time and ELM frequency

From Fishpool, *Nucl Fusion* 38, 1373 (1998).

H89 and H93 confinement enhancement on JET

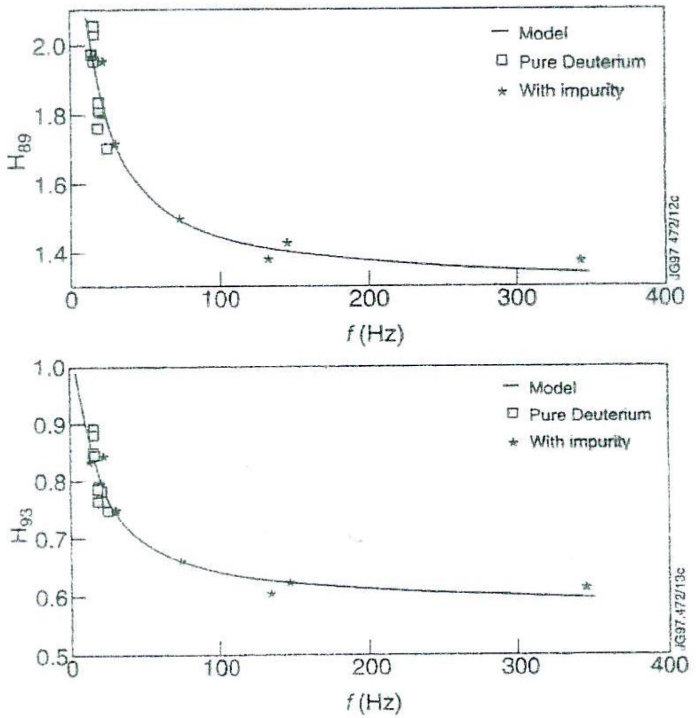

ELM frequency

Confinement in ELMing Regimes (JET)

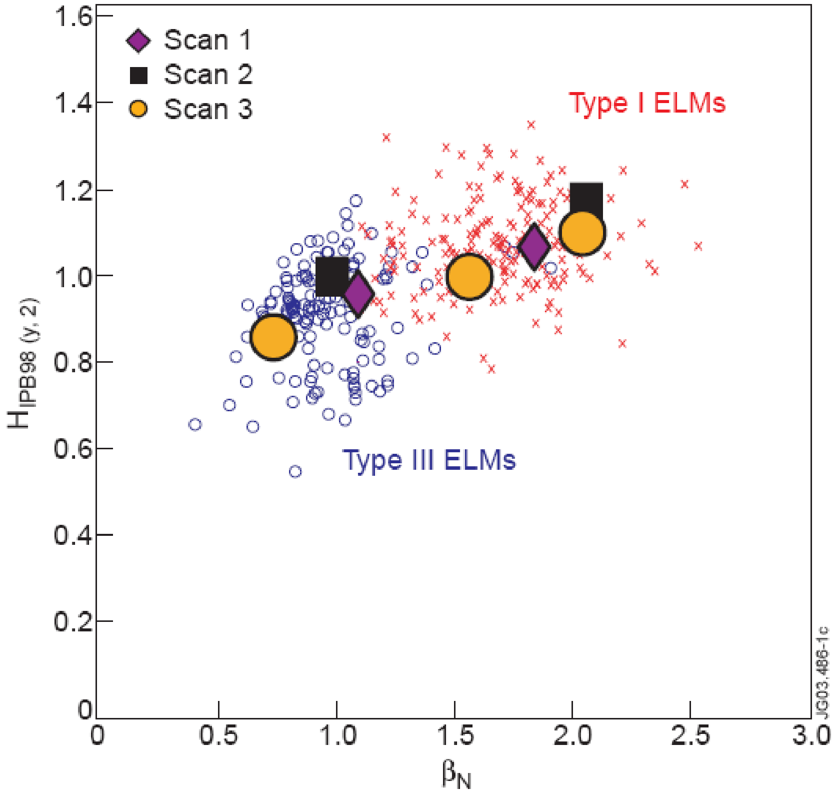

Fig. 2.13. Consistency of the energy confinement with the IPB98(y,2) scaling. $H_{IPB98(y,2)} = \tau_E / \tau_{IPB98(y,2)}$. Data is taken from gas fuelled, NBI and ICRH heated, JET stationary ELMy H-modes from 1994-2001 (red crosses for Type I ELMy H-modes, blue circles for Type III ELMy H-modes) with three dedicated β scans overlaid. Each scan is represented by a different symbol (purple diamonds, black squares or orange circles) and has different values of ρ^* and ν^*, for a range of β .

Filaments

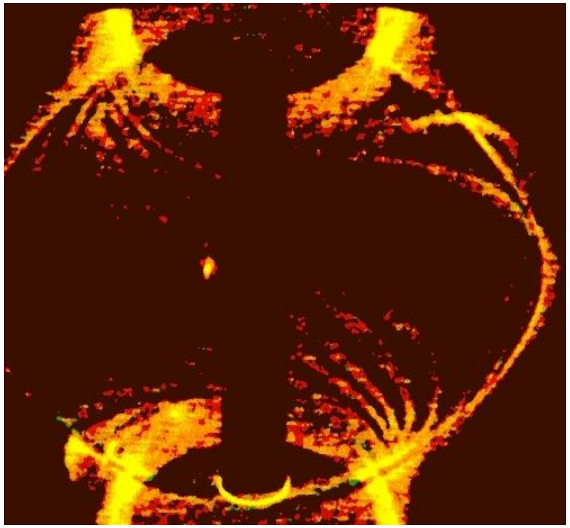

MAST: clear evidence for filaments during ELMs (*Kirk, et al 2004*)

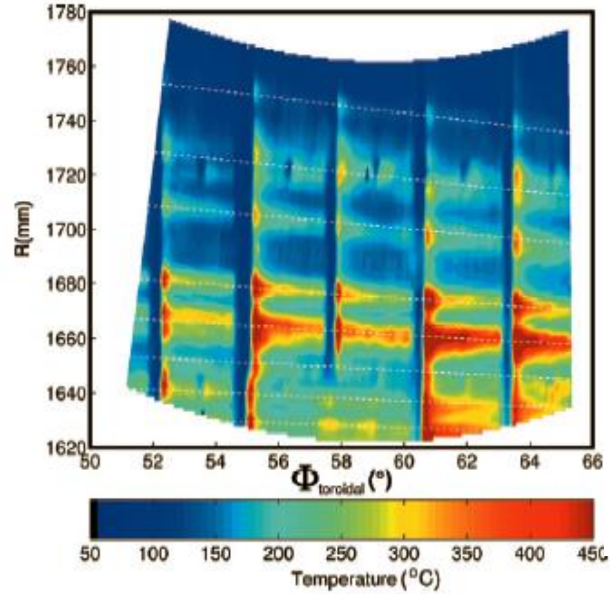

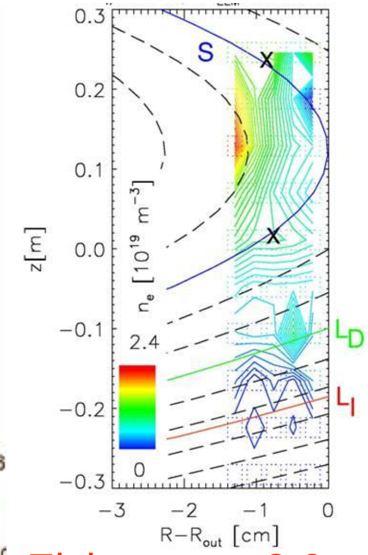

Eich, poster 2.6

ASDEX-Upgrade: stripes on target plate and structures in TS consistent with flux bundles ejected from core (*Eich, et al 2004/2005, Kurzan, 2005*)

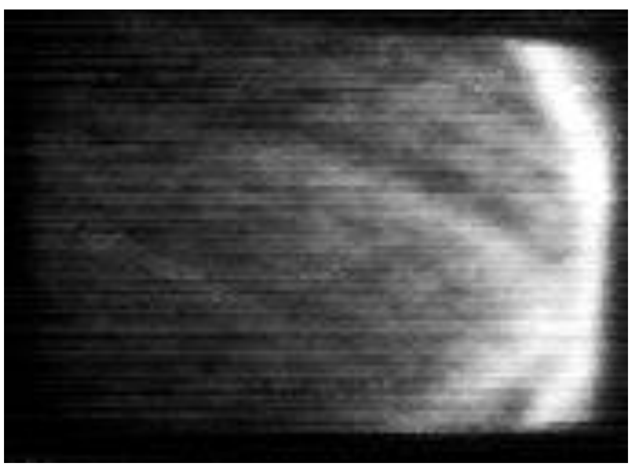

DIII-D: filaments detected in CIII emission (*Fenstermacher, 2004*)

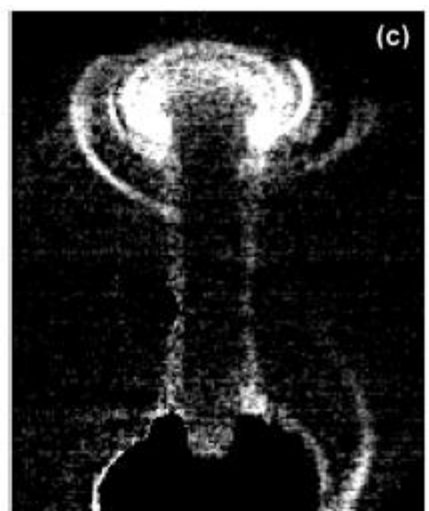

Filament associated with small Type V ELM on NSTX. (*Maingi, et al 2005*)

SOL Structure: MAST

- Images taken of MAST "spherical tokamak" with fast visible camera (A. Kirk, S. Lisgo, UKAEA)

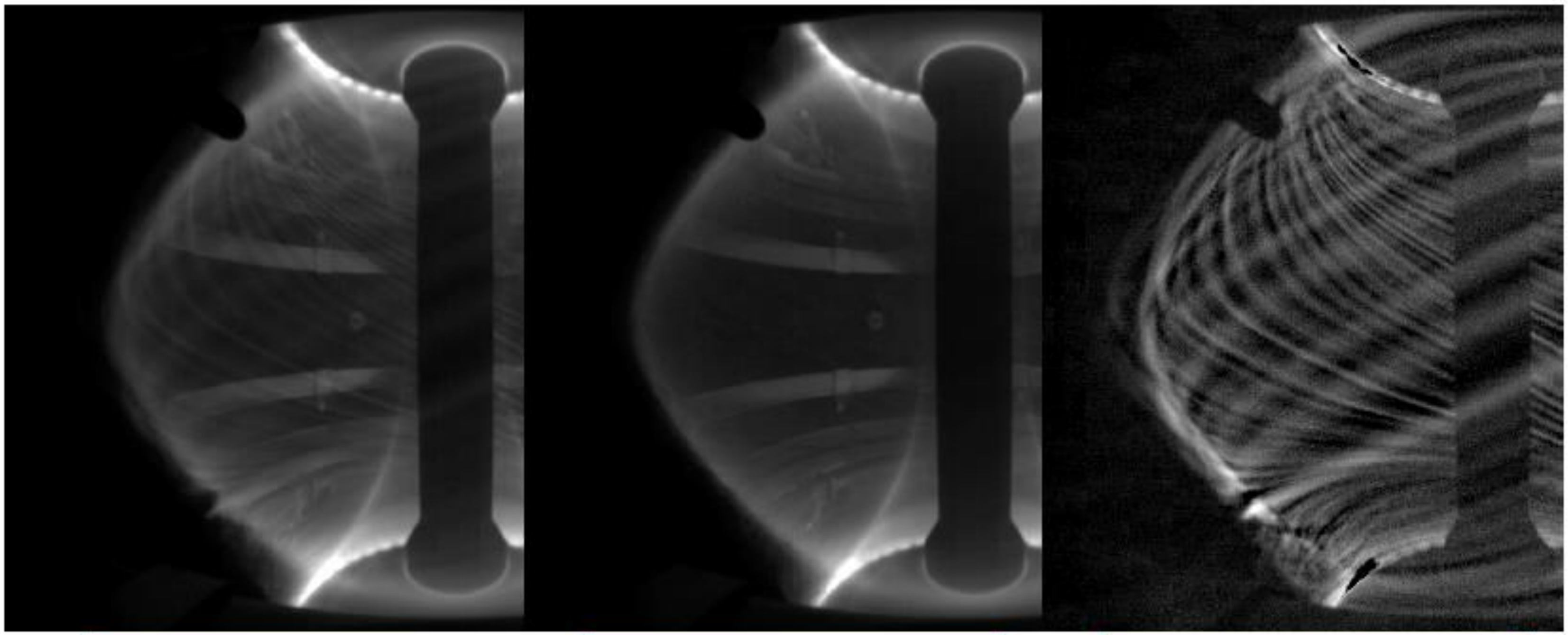

Raw image

Pixel minima on 20 surrounding frames

Minima subtracted from raw image

Filaments in JET
Slow visible camera images

- can see footprint of helical flux tubes

(first reported by Ph. Ghendrih PSI 2002)

69481 various ELM's

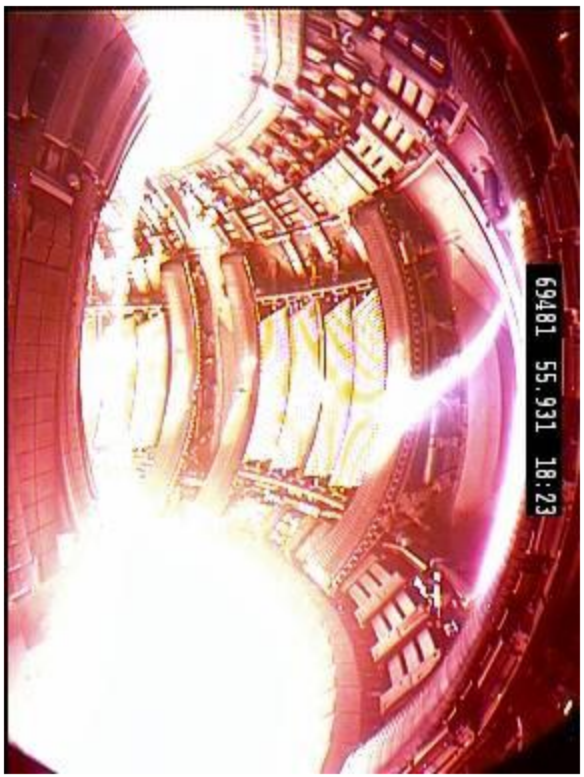

Viewed from Octant 4

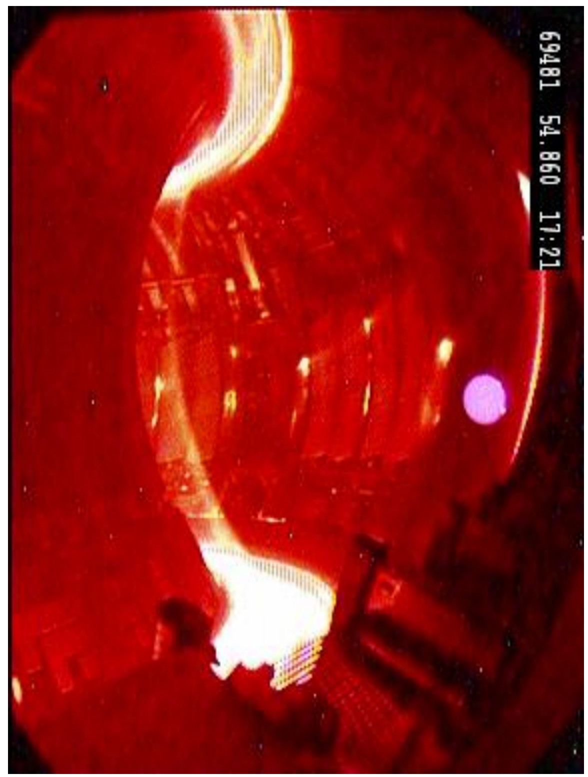

Viewed from Octant 8

JET Fast Visible Camera

Reference view of vessel

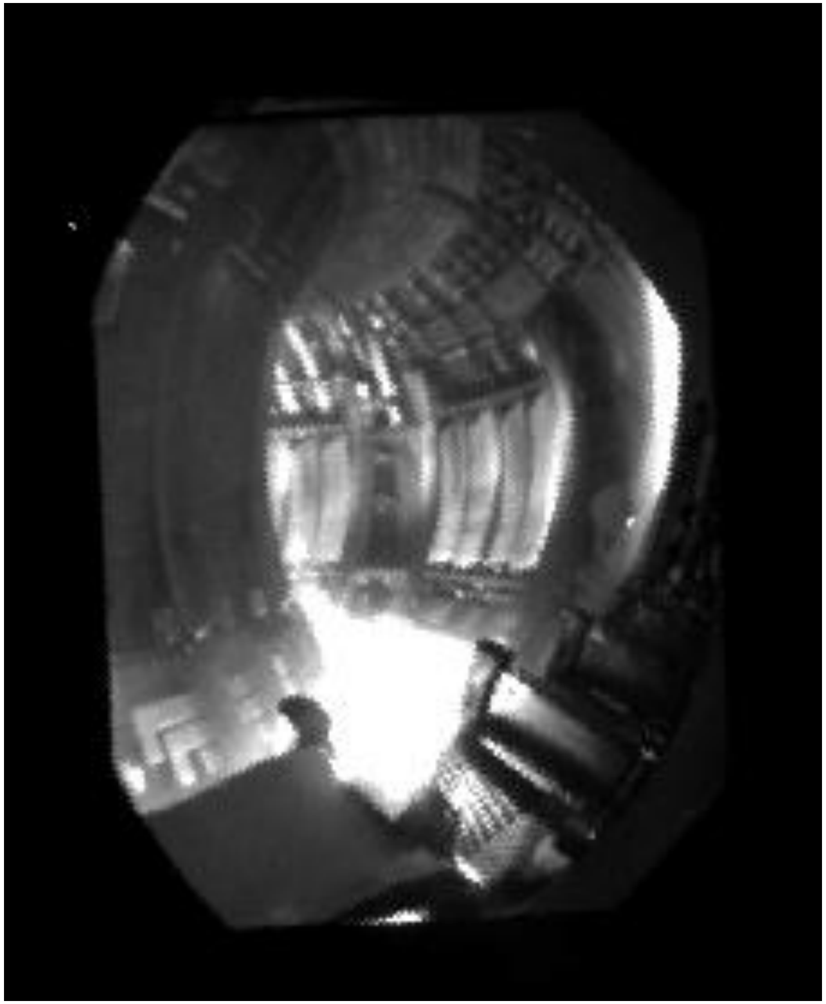

CIEMAT diagnostic

Ref to A. Alonso's EPS poster

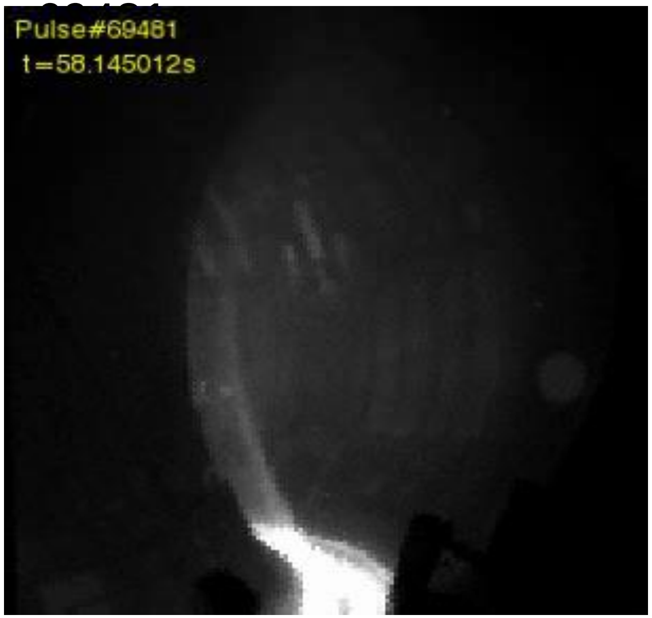

A ~ 1MJ ELM, recorded at 3000 frames/s

(clip covers 100msec)

SOL Structure: MAST

- Images taken of MAST "spherical tokamak" with fast visible camera (A. Kirk, S. Lisgo, UKAEA)

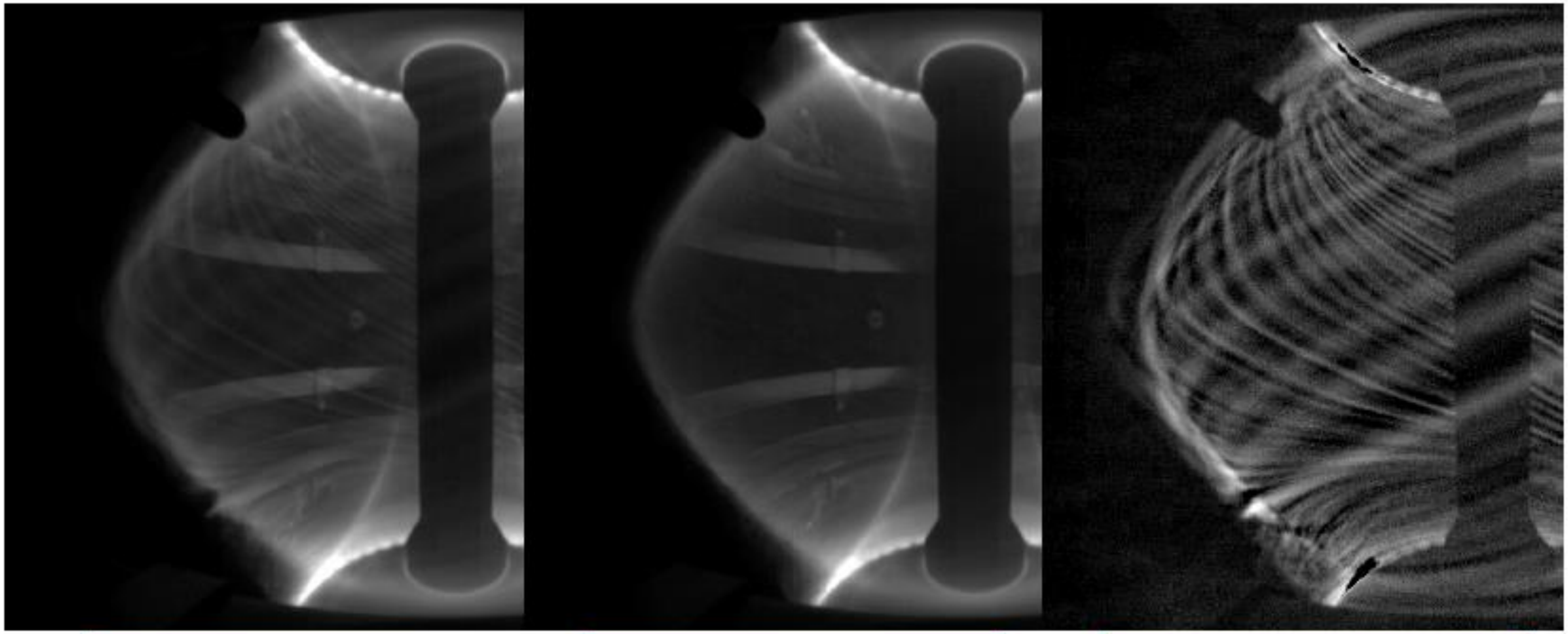

Raw image

Pixel minima on 20 surrounding frames

Minima subtracted from raw image

JET Fast Visible Camera

Reference view of vessel

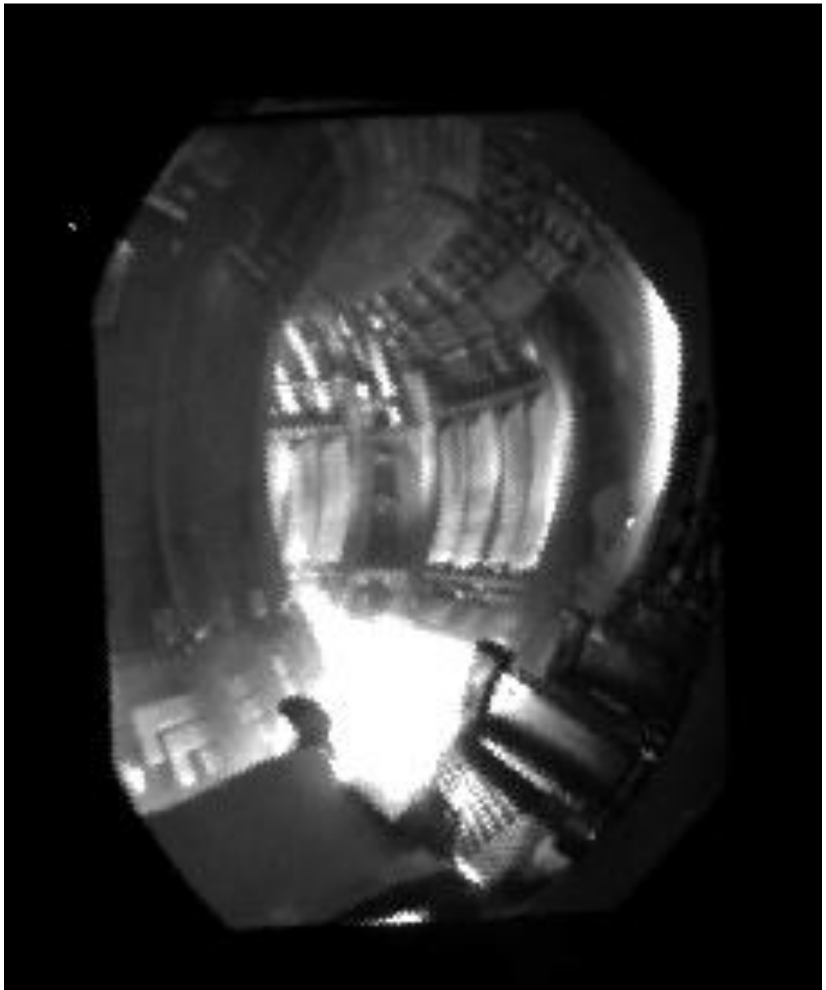

CIEMAT diagnostic

Ref to A. Alonso's EPS poster

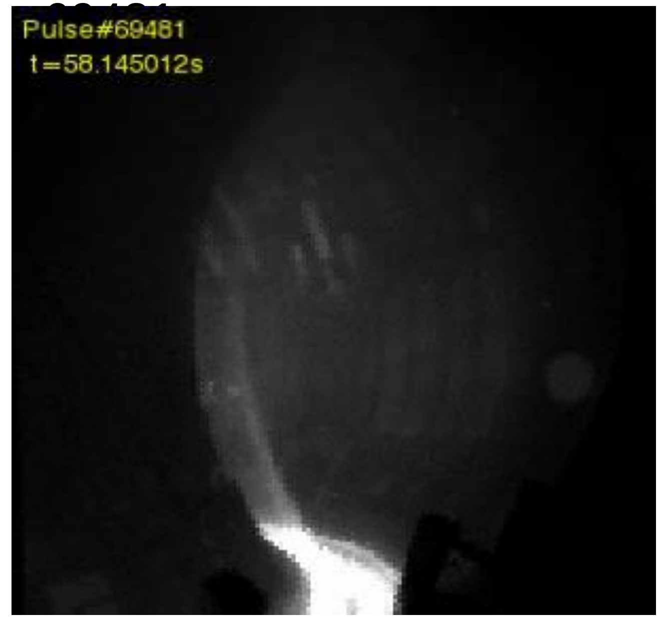

A ~ 1MJ ELM, recorded at 3000 frames/s

(clip covers 100msec)

ELMing H-Mode

Regimes

ELM Types

- Type I ELMs
- Type II ELMs
- Type III ELMs
- Type IV ELMs
- Type V ELMs
- Grassy ELMs

Type III and Type I ELMs

MAST

Increasing P_{NBI}

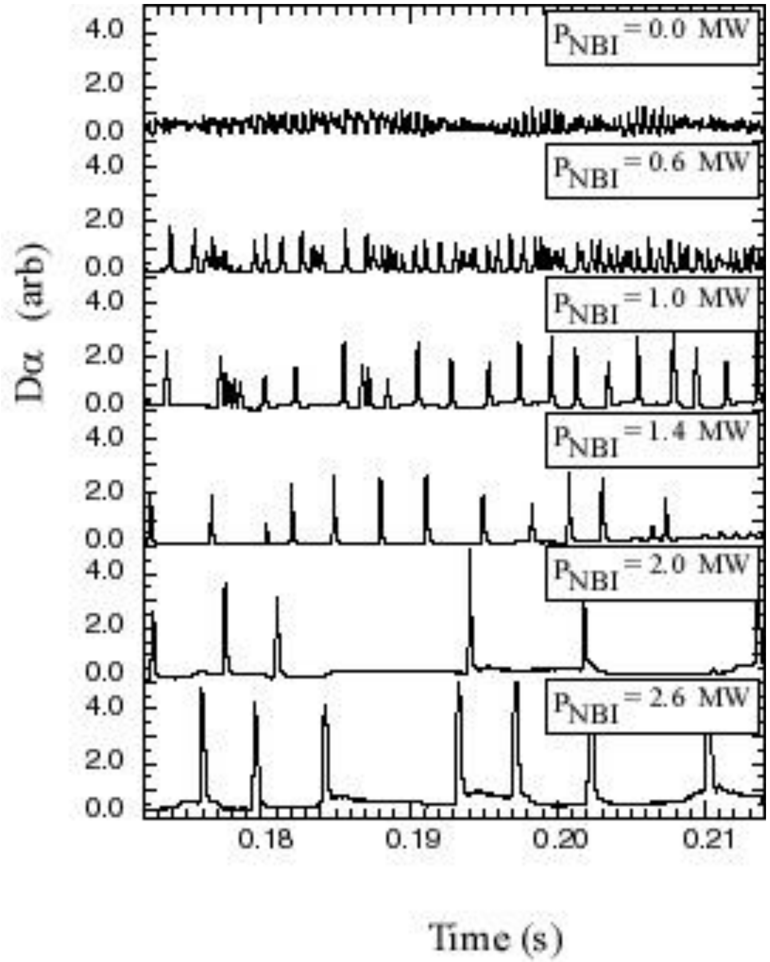

Typical dependence of ELM frequency and type on input power

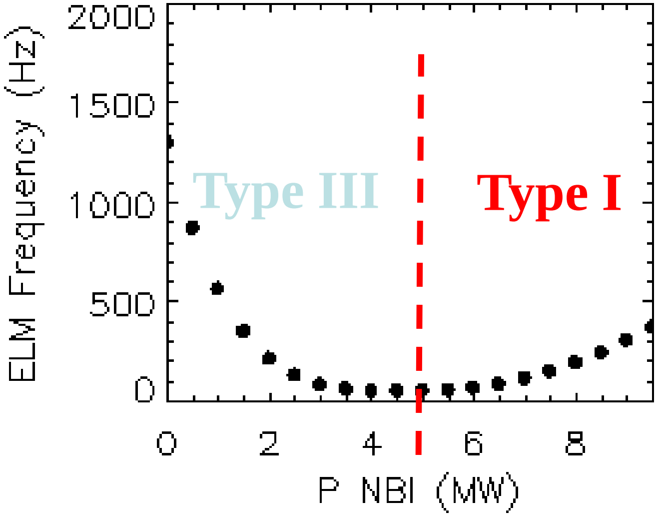

Transition when $P_{in} \sim 1.5\text{-}2{*}P_{L\text{-}H}$

Operating Diagram

- n_{edge}-T_{edge} diagram

ASDEX Upgrade (W Suttrop et al)

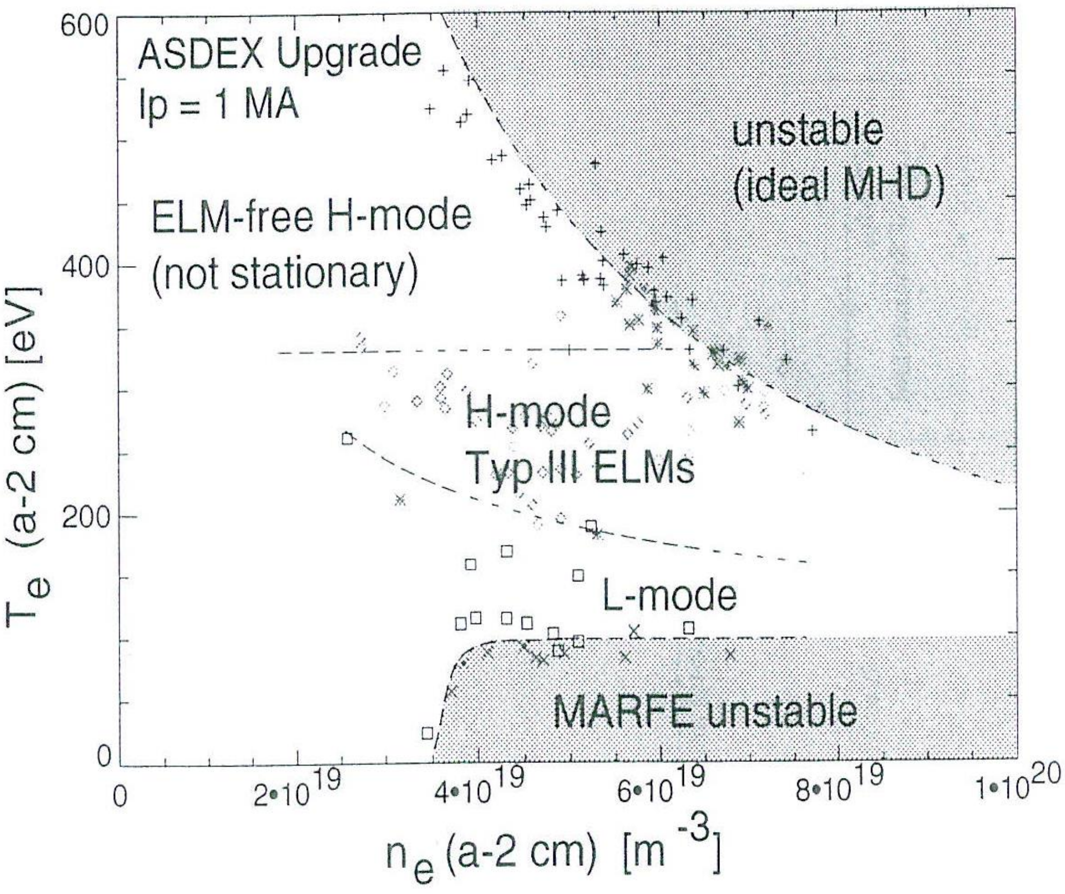

Type III ELMs

- Higher ELM frequency
- Smaller energy loss per ELM
- Reduced confinement (10 - 30 %)
- Type III ELMs are observed below a critical pedestal temperature

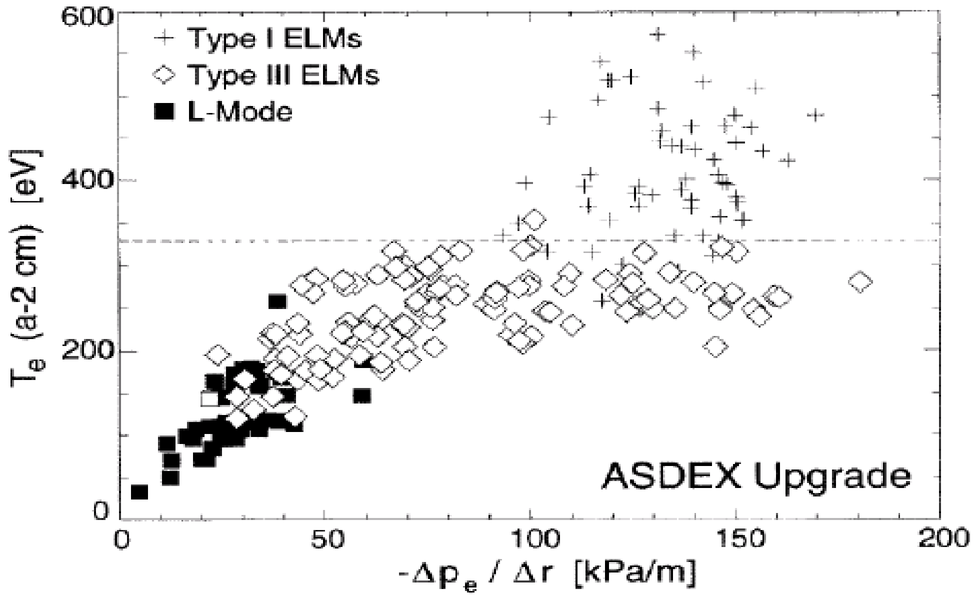

T_{crit} tends to increase with toroidal field

Type III ELMs

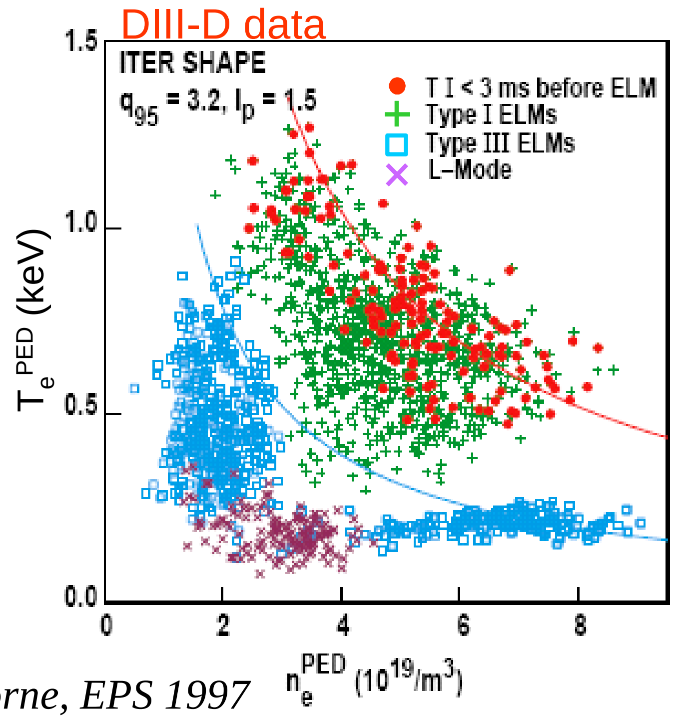

T Osborne, EPS 1997

The low n_e-high T_e branch of Type III was originally called type IV

Whether Type III ELMs at low and high collisionality are due to the same physics mechanism is still an open question

Precursors to Type III ELMs

Type III : more clearly associated with precursors

	n	m	Δr (cm)	$f\,(kHz)$	$\tau(\mu s)$
JET DIII-D	$\geq$ 8 5 – 10 (low n_e 6-13)		10	50-100 (multiple 50-80)	250
ASDEX Upgrade	10-15	15-20	4	100 (counter) 60 (co); sometimes 2 modes 100, 200	
C-MOD COMPASS-D	> 5	> 10 13		150 70-120	$\lesssim$ 50 $\lesssim$ 200
TCV JFT-2M	5-8			120 $\downarrow$ 70 250 $\downarrow$	50 20

Transient Losses due to Type III ELMs

Type III

	$\delta W\%$	$\delta N\%$
ASDEX Upgrade	0.5 – 2	
DIII-D	1 – 5	
COMPASS-D	1	
TCV	2.5	2

Type II ELMs

- Small energy loss per ELM
- Requires proximity to double null and highly shaped plasmas
- High p_{ped}, (confinement ~like Type I ELMs)
- Low T_e^{ped} (T_{ped}(Type II)~T_{crit}(Type I->III transition))
- Broadband MHD activity
- But for narrow operational window and high n/n_G ~0.5-1
- Type I and Type II often co-exist

Grassy ELMs

• **Small ELMs at high confinement mainly seen on JT-60U**

• **β_p is the critical parameter, although high δ and q_{95} also required**

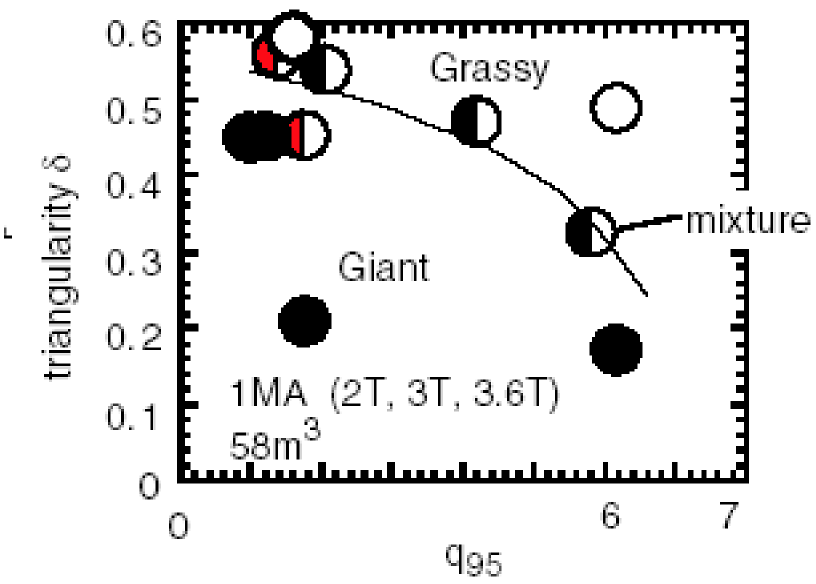

Grassy ELMs - Effect of Toroidal Rotation

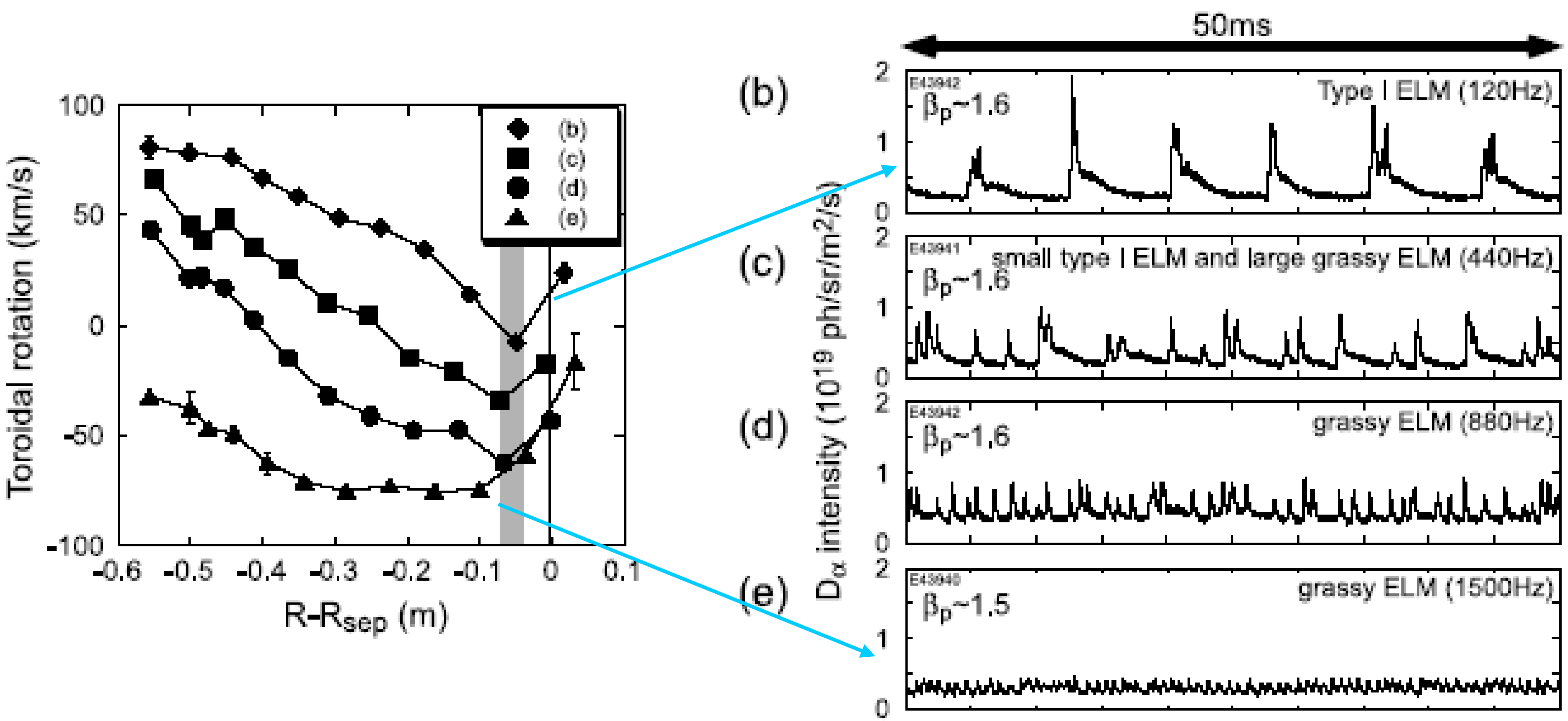

Type V ELMs

- Observed on NSTX
- Similar to EDA/HRS (see later) but no mode observed
- High pedestal collisionality, $n/n_G > 1$

Type I ELMs

Characteristics

Type I ELMs

- Observed on many machines when $P > 1.5\text{-}2{*}P_{LH}$
- ELM crash occurs on very fast timescales, of the order of 100-300μs
- The pedestal, both n_e and T_e build up again, until the next ELM occurs on a much longer time scale.

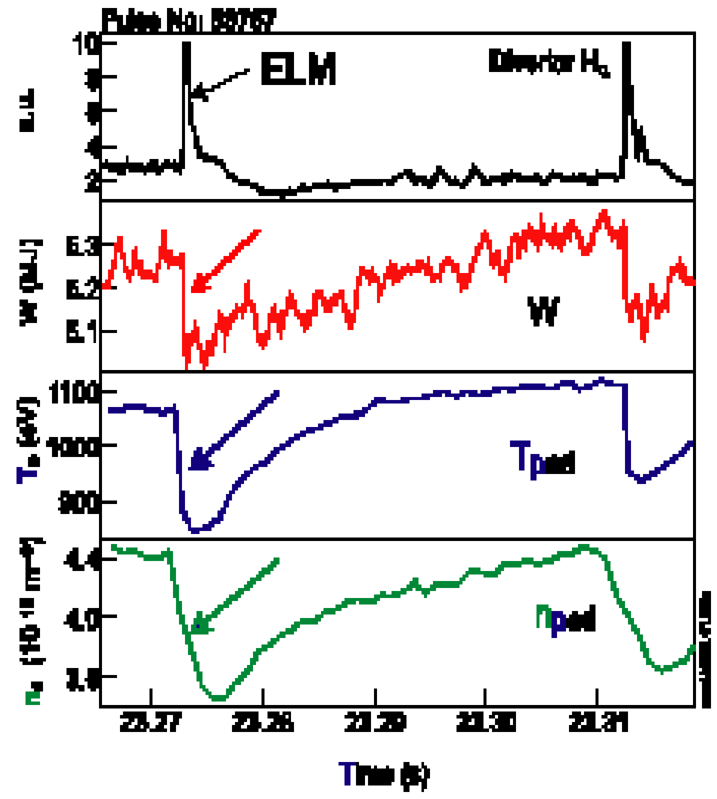

Precursors to Type I ELMs

Type I : (or 'large type III' – COMPASS-D, TCV?)

	n	m	Δr (cm)	$f\,(kHz)$	$\tau(\mu s)$
JET?	0 – 4		5	15	100
ASDEX Upgrade	5 – 10	16-15	1 – 2	20 counter (2 frequencies) ? Co*	10^3
COMPASS-D	3 – 8 (4,5)	 (9,14)	1 – 2	70-120 (Ohmic) 140-200 (ECRH) (93,116)	 <10^3
TCV*		16-20		50	50

Transient Losses due to Type I ELMs

Type I $$\delta W \sim \Delta R^2 p'_{crit}$$

	$\delta W\%$	$\delta N\%$
JET ASDEX Upgrade DIII-D COMPASS-D* TCV* JTF-2M • Large type III?	2 – 9 3 – 6 1 – 7 3 – 4 3 – 12	1 – 5 3 3 - 7 5

Type I ELMs

Thomson scattering (TS)

The comparison of the ELM density collapse at low and high field side indicates that the ELM crash occurs first in the low field-side of the tokamak

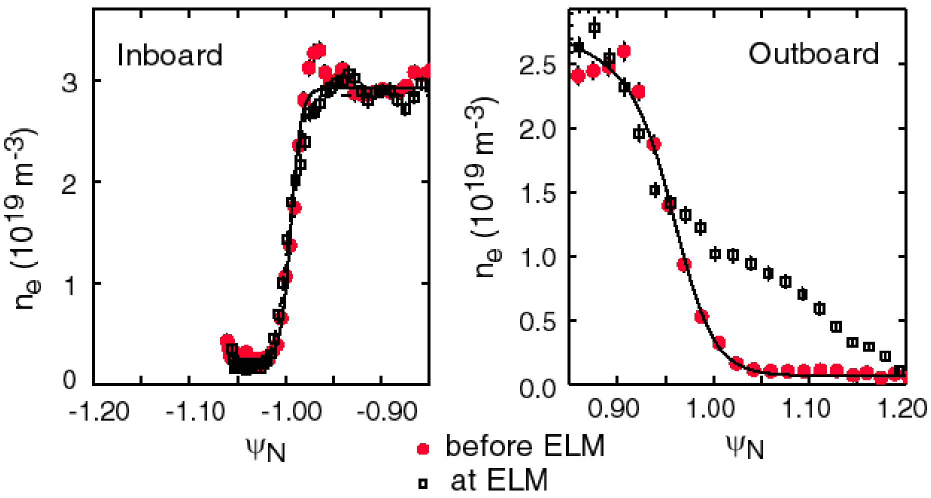

ELMs are characterised by ballooning-like behaviour

Type I ELMs

The density perturbation propagates to the inboard side at ~ ion sound speed.

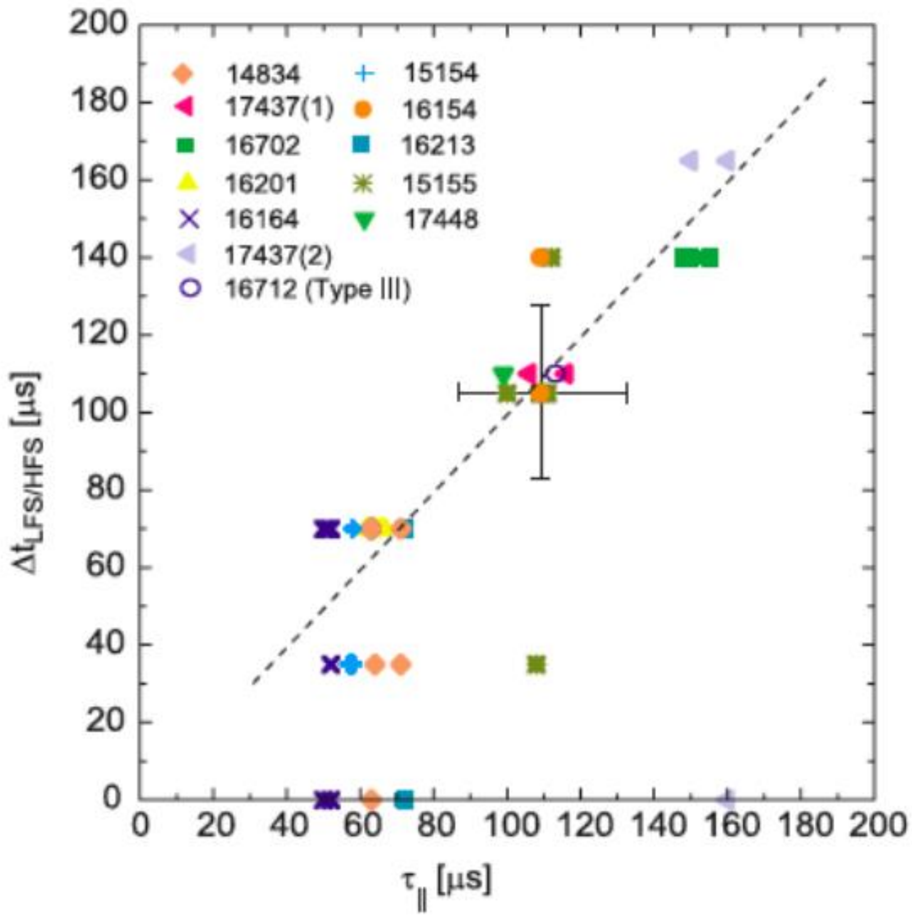

Theory Models

Theory Models

Issues

- Trigger
- Fast non-linear phase
- Exhaust of plasma
- Recovery and repetitive cycle

Outcomes from developing ‘understanding’

- Identify regimes with tolerable ELMs
- Suggests control means

Standard" ELM-model

(Connor, Hastie, Wilson, Miller, PoP, 1998)

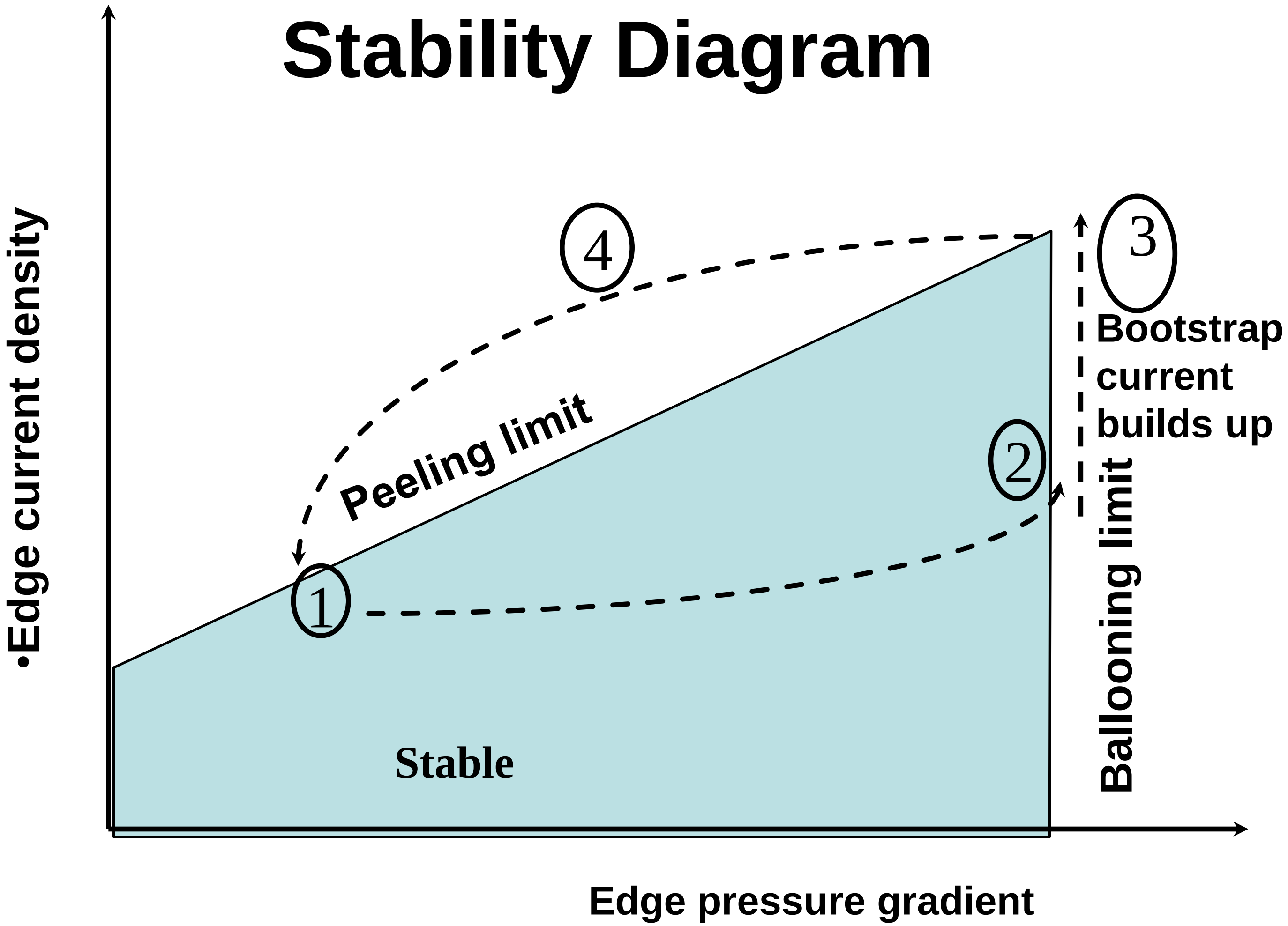

Type I ELM cycle

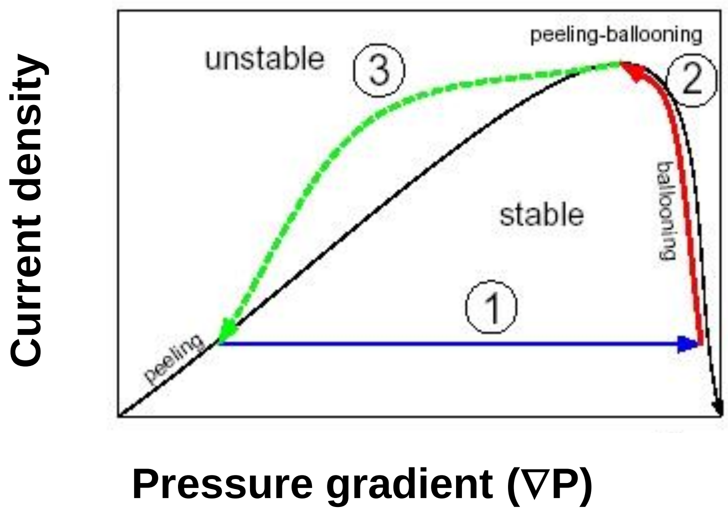

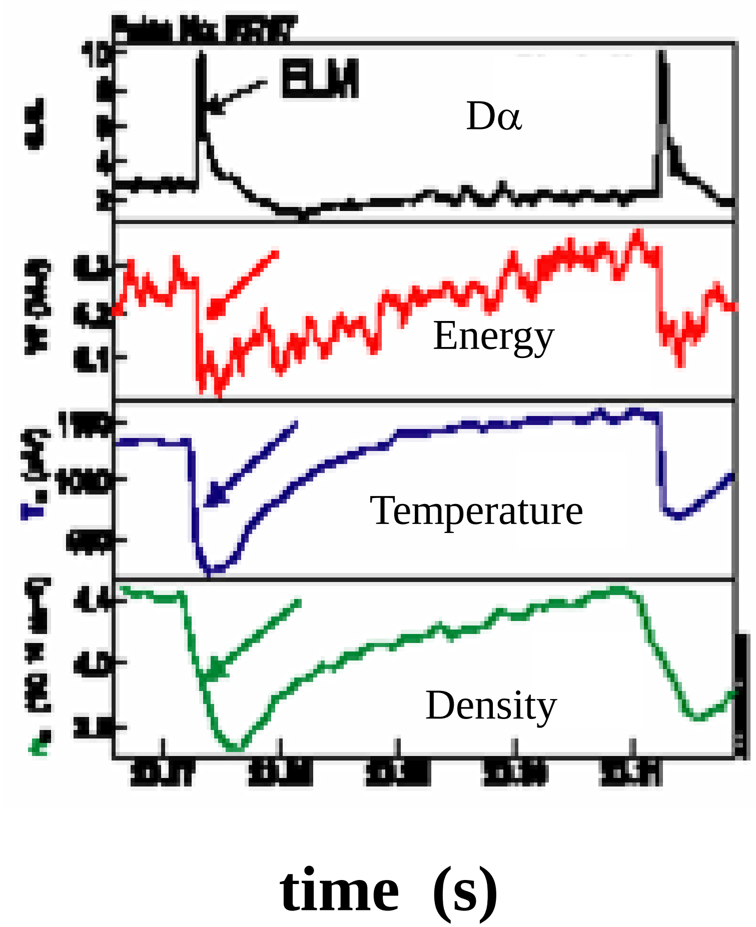

1. ∇P rises on transport time scale
2. ∇P clamped by high-n ballooning
   - edge current density rises on resistive time scales
3. Medium n instability
   - p and j lost until stable again

What triggers the ELM? Type I ELMs

- We believe the Type I ELM is triggered by peeling-ballooning modes
  - Comparison of linear stability threshold with observed profiles at ELM onset shows good agreement - Note current (j) = 2- shear (s):

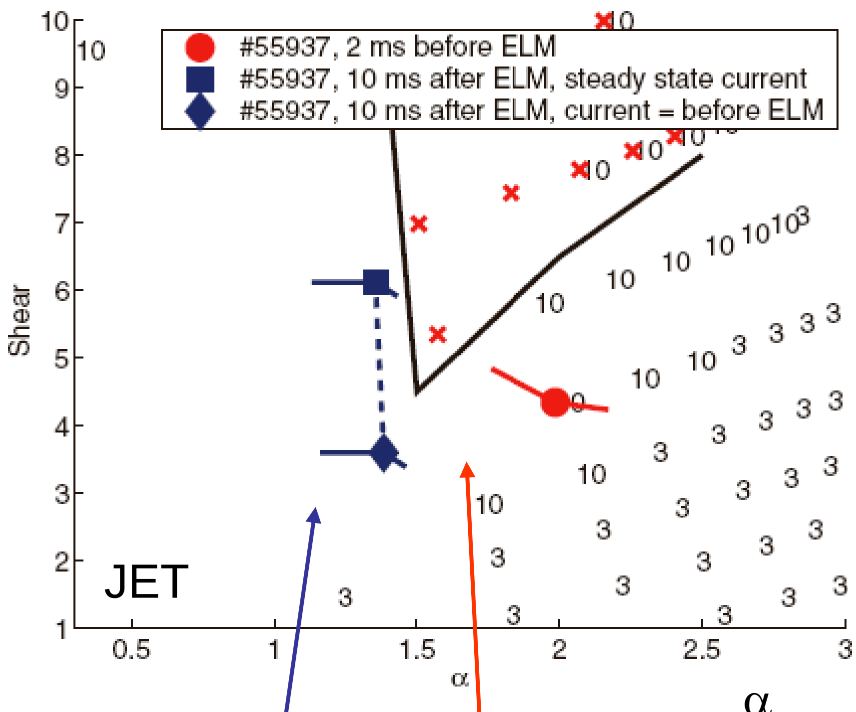

After ELM:
Stable (2 assumptions about current)

Before ELM:
unstable

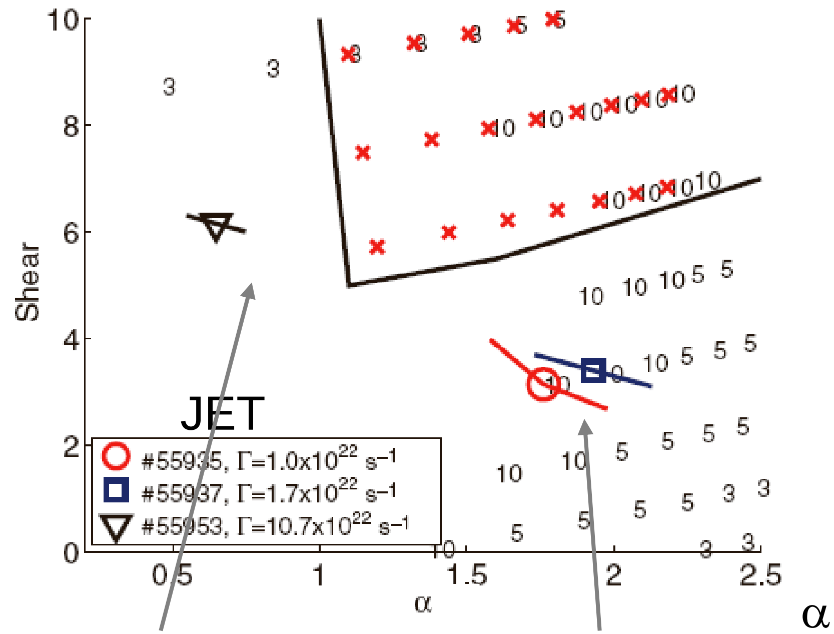

Increase gas-puffing
⇒ Type III ELMs
⇒ Below peeling-ballooning

Type I ELMing:
unstable

Linear MHD Theory

- **Ideal MHD instabilities in the pedestal:**
  - ballooning modes
  - peeling modes
- **There are two main drives for ideal MHD instabilities:**
  - pressure gradient ⇒ ballooning modes
  - current gradient ⇒ kink, or peeling, modes
- **In the pedestal region, large pressure gradients can build up**
  - ⇒ directly drives ballooning modes
  - ⇒ drives bootstrap current ⇒ kink, or peeling, modes
- **Theoretical codes (ELITE, GATO,MISHKA) exist that can scope out the allowed operating regions**
- Most modelling employs limiter geometry approximations
- How accurately does this represent the true separatrix geometry?

Stability Trends

Stability if $$\alpha\left[D - s\Delta'_{Sh}\right] > \frac{Rqs}{B} j_{\square}$$

$$j_{\square} = j_{ohmic} + j_{Bootstrap}; \; j_{Bootstrap} \sim \alpha f\left(\nu_{*e}\right)$$

$$\alpha = -\left(2Rq^2/B^2\right)\left(dp/dr\right);$$

$$D = \varepsilon\left(1 - \frac{1}{q_a^2}\right) - \text{'magnetic well'}$$

Implications

- $\nu_{*e} \downarrow \Rightarrow j_{Bootstrap} \uparrow \Rightarrow \text{destabilising}$
- current ramp down $\Rightarrow \text{stabilising}$

Different radial mode structures exist in different regimes

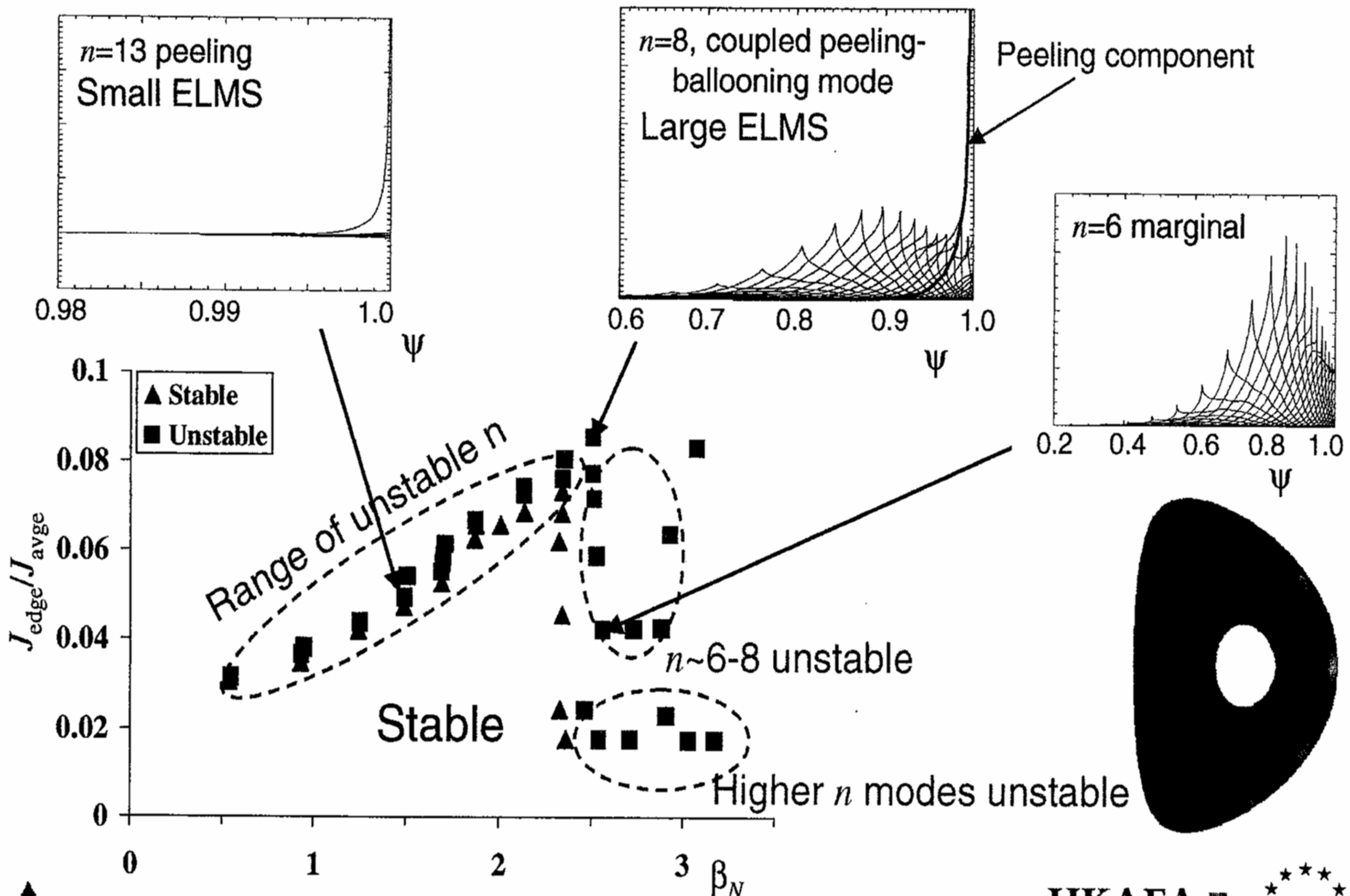

Rotation

Flows below sound speed only affect highest mode numbers

- Toroidal flow shear has been incorporated into ELITE (high flow shear, but flow<<sound speed)

- Stabilising effect on the highest *n* modes, but negligible influence on modes responsible for ELMs: sonic flows may have an impact
  - more important in STs, where rotation is higher (and sound speed can approach Alfvén speed)
  - effect of flow shear on non-linear evolution is an open question

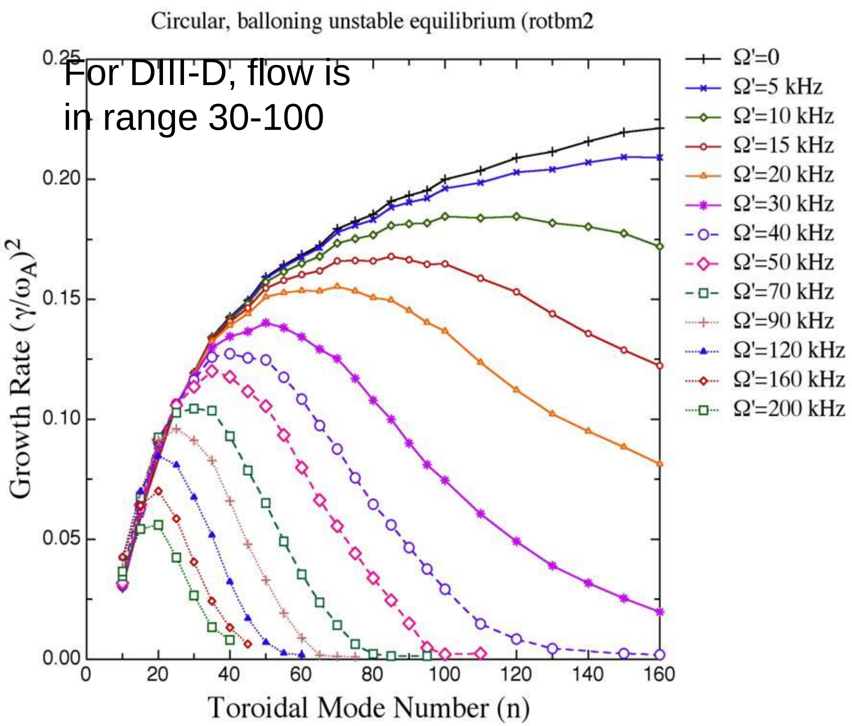

Snyder, 2005

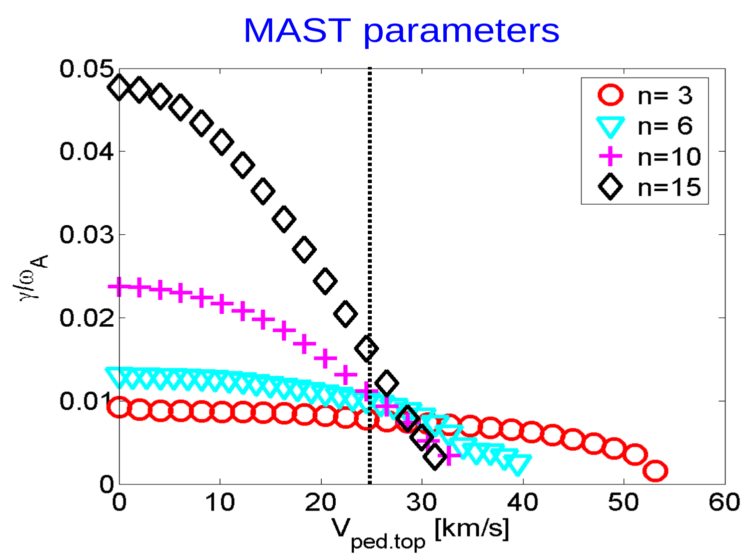

Saarelma, 2005

Diamagnetic Effects
- do they affect MHD model?

- **Diamagnetic effects are likely to be important in the pedestal**
  - **predicted to stabilise ballooning modes when** $\frac{\omega_*}{2} > \gamma$ $\omega_* = \frac{nq}{2r}\rho_i v_{th,i}\frac{1}{n_i}\frac{dn_i}{dr}$
  - **usually only gives small quantitative difference in practice**

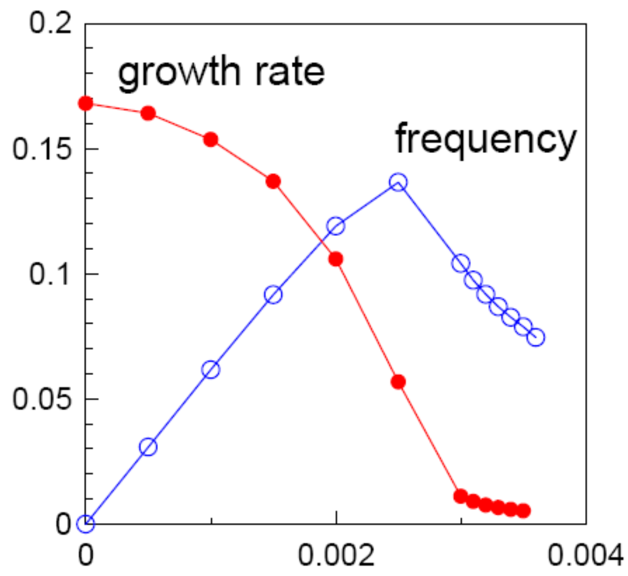

Increasing ω_* ⟶

Huysmans, 2001

Snyder, 2002

Role of Diamagnetic Stabilisation

- **Diamagnetic effects are important when** $\omega_* > 2\gamma$

n=toroidal mode number
ε=inverse aspect ratio
β_θ=poloidal beta
ρ_i=ion larmor radius
Δ=pedestal width
$\omega_A = v_A/Rq$

  – **This becomes**

$$q\sqrt{\beta_\theta} > \frac{2\Delta}{n\rho_i}\frac{\gamma_0}{\omega_A} \sim 5$$

~5 for Δ~30ρ_i
n~10

Expect ~1 for large ELM in explosive phase

- **Diamagnetic stabilisation of most dangerous *n* ~10 modes occurs at higher poloidal β - also a role for *q*, depending on pedestal scaling with r*i*.**
  – **could this explain some small ELM regimes?**

Impact of the Separatrix

Some progress numerically:

– KINX code (*Medvedev*) higher current density required to trigger kink modes

TCV ELMs

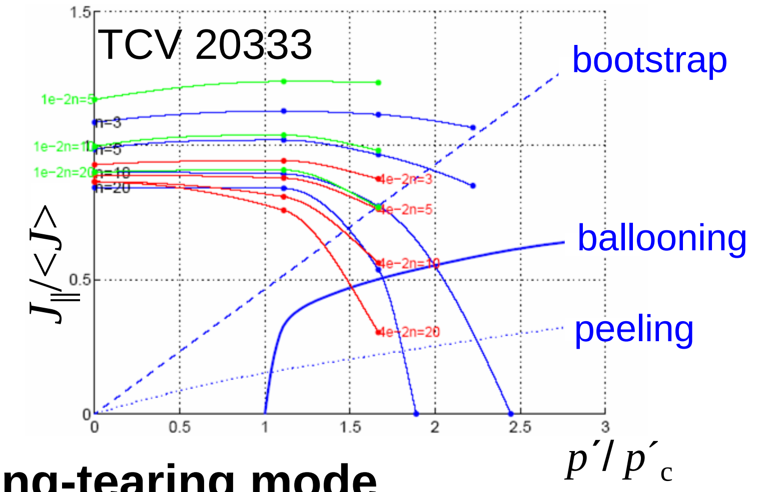

New JOREK code (*Huysmans*) predicts new peeling-tearing mode

- **mode has tearing structure near X-point**
- **growth rate converges as separatrix geometry is approached**
- **growth rate not sensitive to small changes in *q***

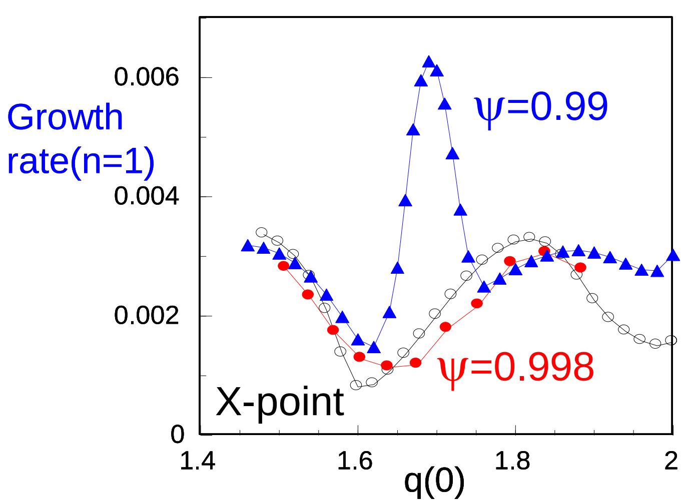

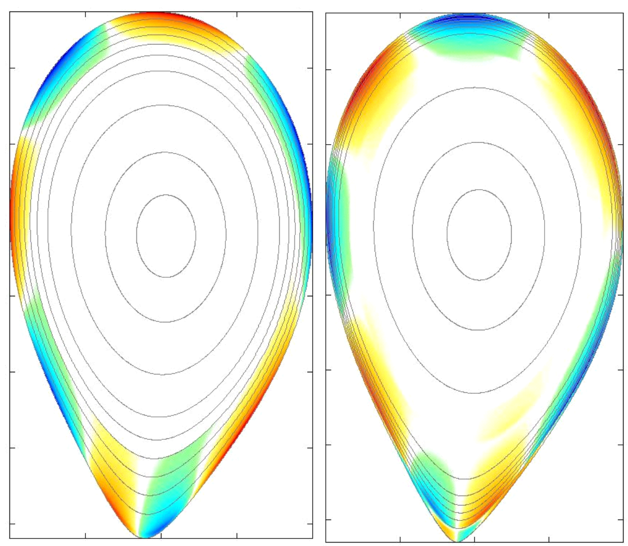

peeling mode

peeling-tearing mode

Type III ELMs

- **The mechanism for Type III ELMs is less clear than for Type I:**
  - **Low density Type III ELMs could be peeling: but pure peeling modes are very localised**
  - **High density Type III could be resistive ballooning (below critical T_e): but why an explosive event, rather than diffusive transport?**
    - **could resistive ballooning trigger the peeling mode?**
  - **Type III ELMs could also be a consequence of avalanche (e.g. 'sandpile' model) phenomena**

DIII-D data

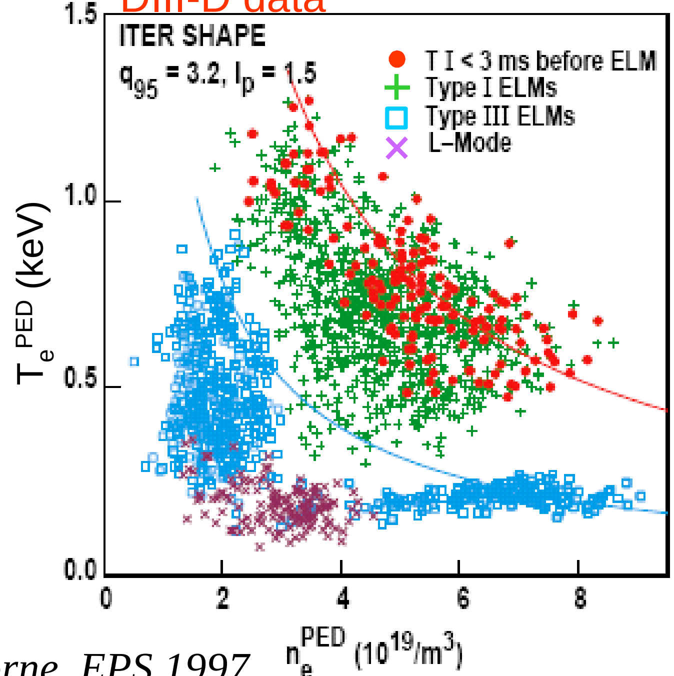

T Osborne, EPS 1997

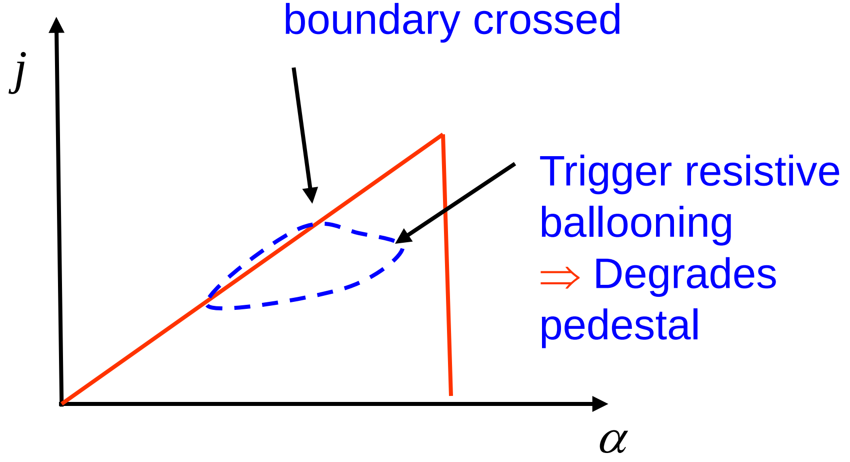

Other Type III ELM Theory Models (1)

- **Chankin-Saibene resistive ballooning model for triggering Type III ELMs compared with JET data**

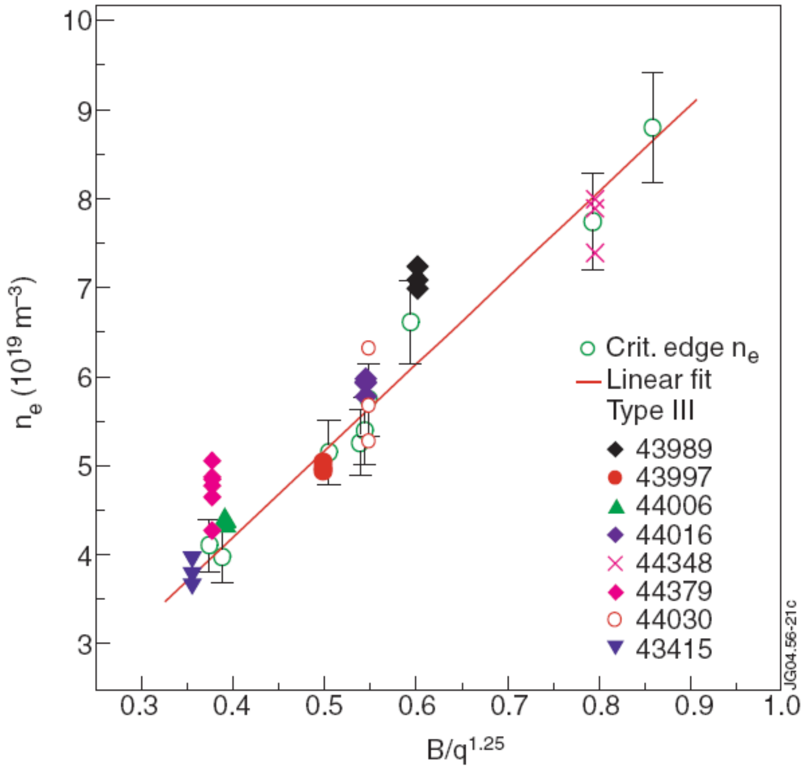

Fig. 4.12. Pedestal density at the Type I-III ELM transition and during Type III ELMs. (From Ref. [105].)

Other Type III ELM Theory Models (2)

- **Pogutse-Igitkhanov resistive interchange model driven by magnetic flutter for triggering Type III ELMs compared with JET data**

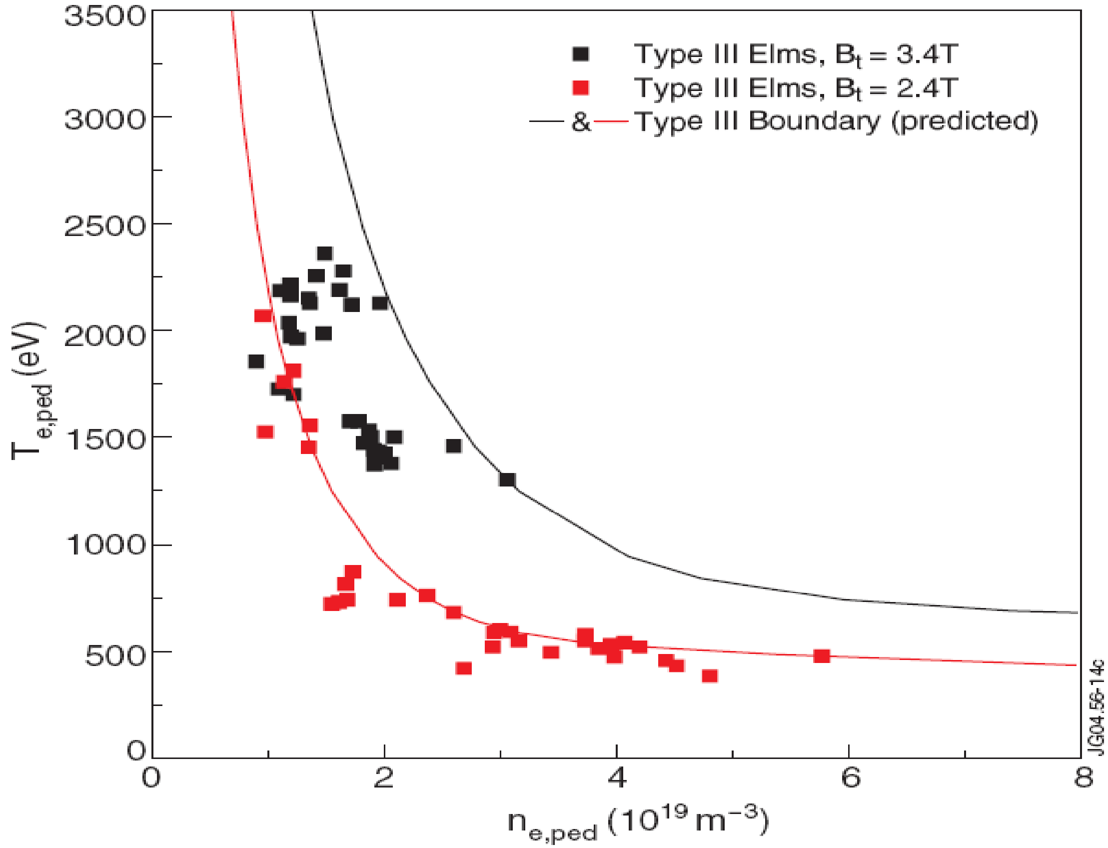

Fig. 4.11. Pedestal $n_e - T_e$ diagram for 2.5 MA/2.4-2.6T and 3.3-3.6MA/3.4T discharges. $n_{e,ped}$ is measured with the FIR interferometer outermost channel and $T_{e,ped}$ with the ECE heterodyne radiometer. The data are compared with the critical temperature (or upper boundary) for Type III ELMs predicted by the model of Pogutse and Igitkhanov [127,128]. (From Ref. [105].)

Power Expelled in an ELM

Target Energy Deposited due to ELM (JET)

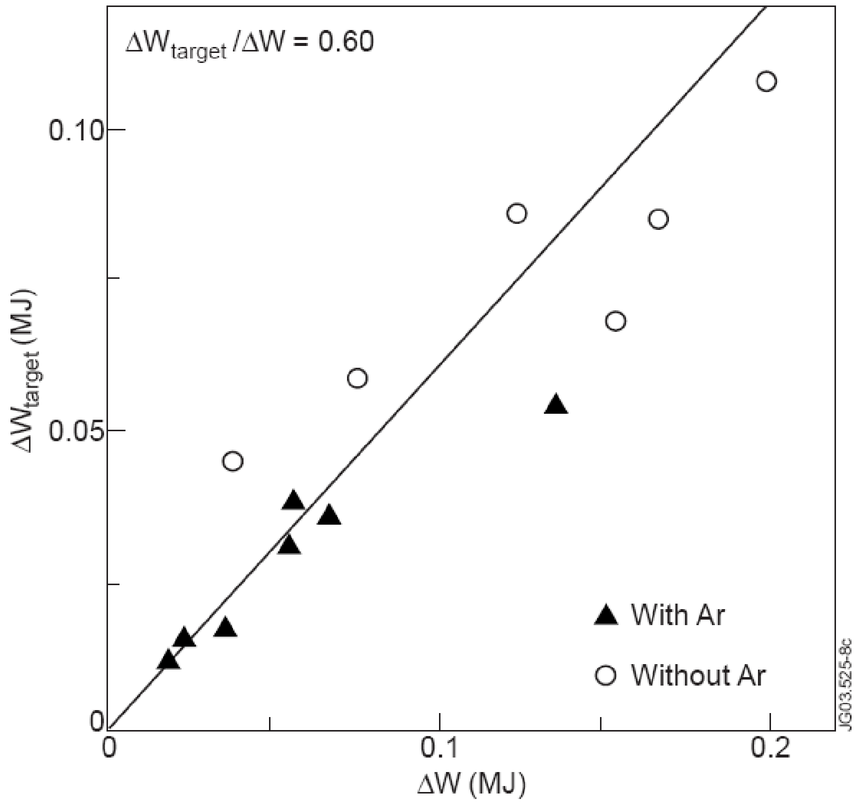

Fig. 7.1. Target energy load due to ELMs, ΔW_{target}, versus energy lost from plasma due to ELMs, ΔW. (From Ref. [214].)

Time Lag to Divertor Target of Main Heat Flux

(Particle-in-cell kinetic calculations show faster high energy electron loss to divertor plates)

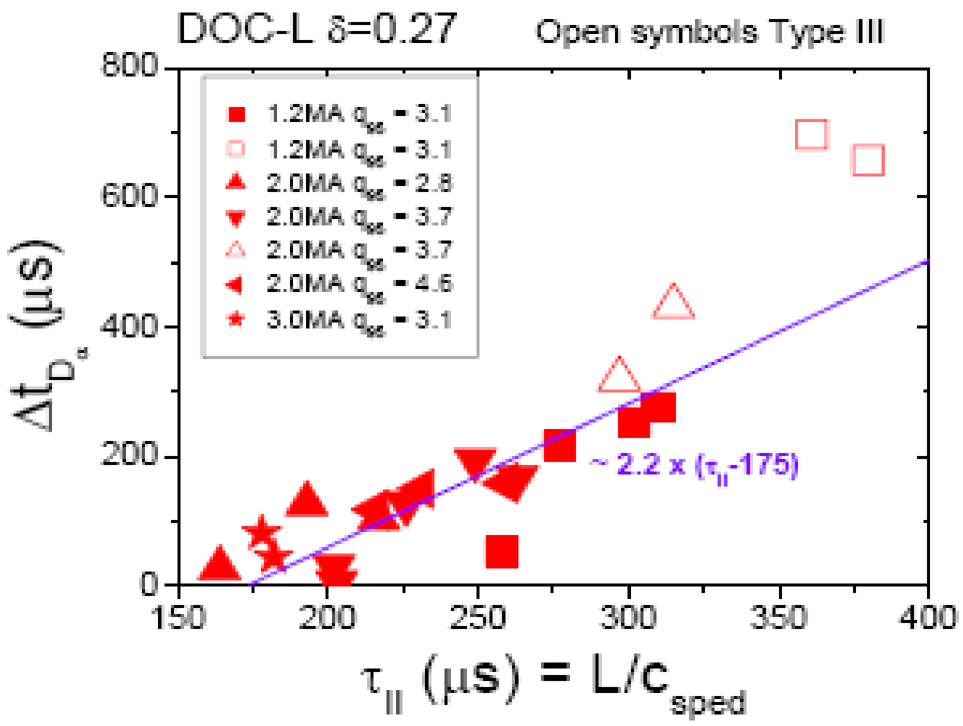

Collisionality Dependence of ELM Energy Loss

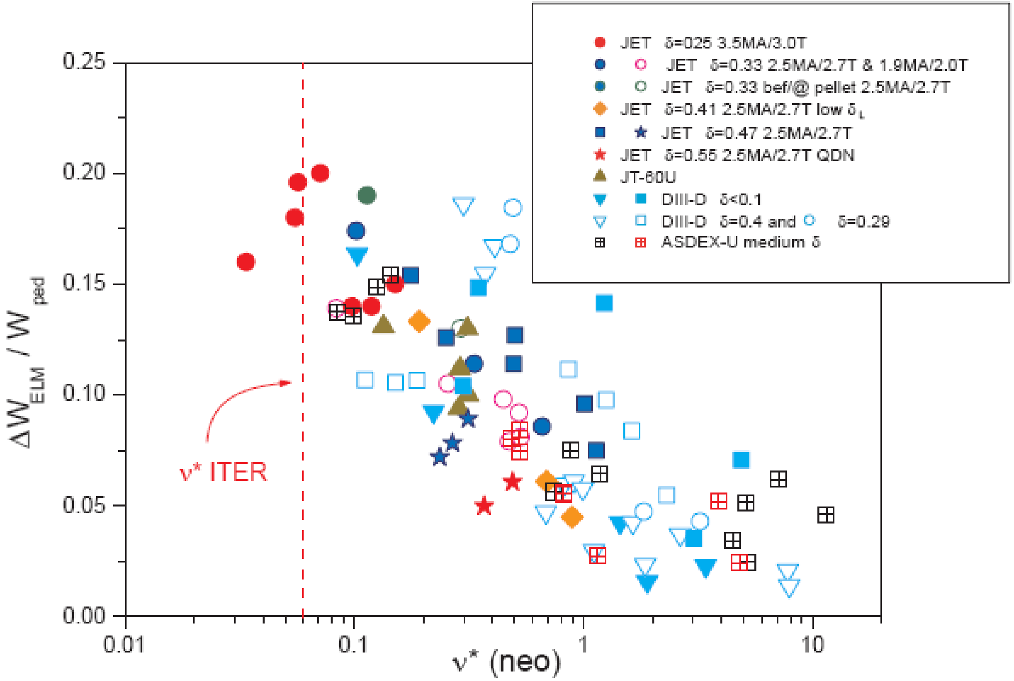

Fig. 5.4. Normalised ELM energy loss ($\Delta W_{ELM}/W_{ped}$) versus pedestal plasma collisionality for a large range of Type I ELMy H-mode plasmas in ASDEX Upgrade, DIII-D, JT-60U and JET including various plasma triangularities, ratios of $P_{INPUT}/P_{L\text{-}H}$, pellet triggered ELMs, and impurity seeded discharges (Ar). (From Ref. [15].)

Theory input - Peeling-Ballooning modes

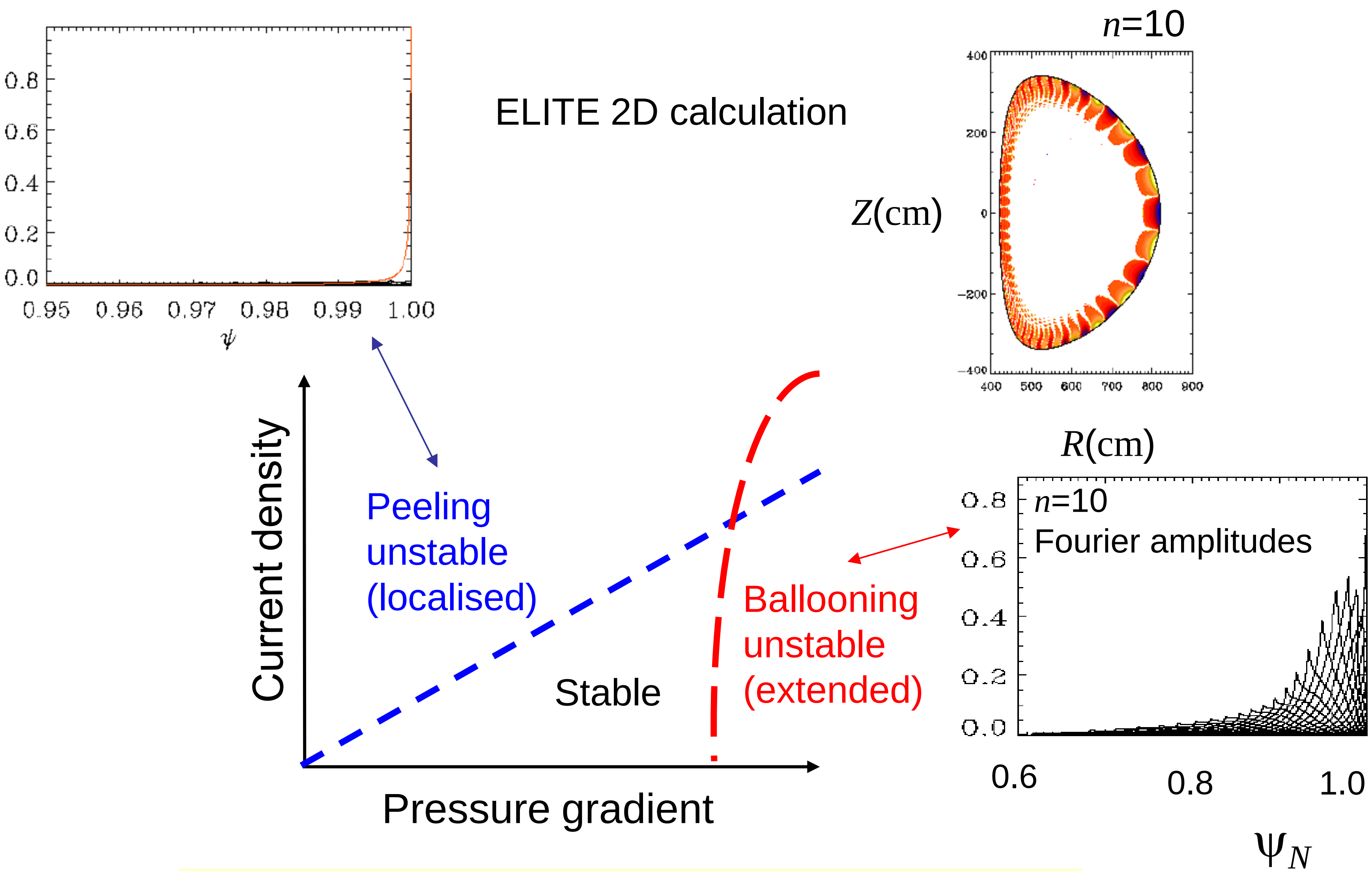

Width of eigenmode determines δW_{ELM}

Peeling-ballooning Modes

Reduced $\delta W_{ELM}/W_{ped}$ at high n_e, n/n_G correlated with reduced mode width

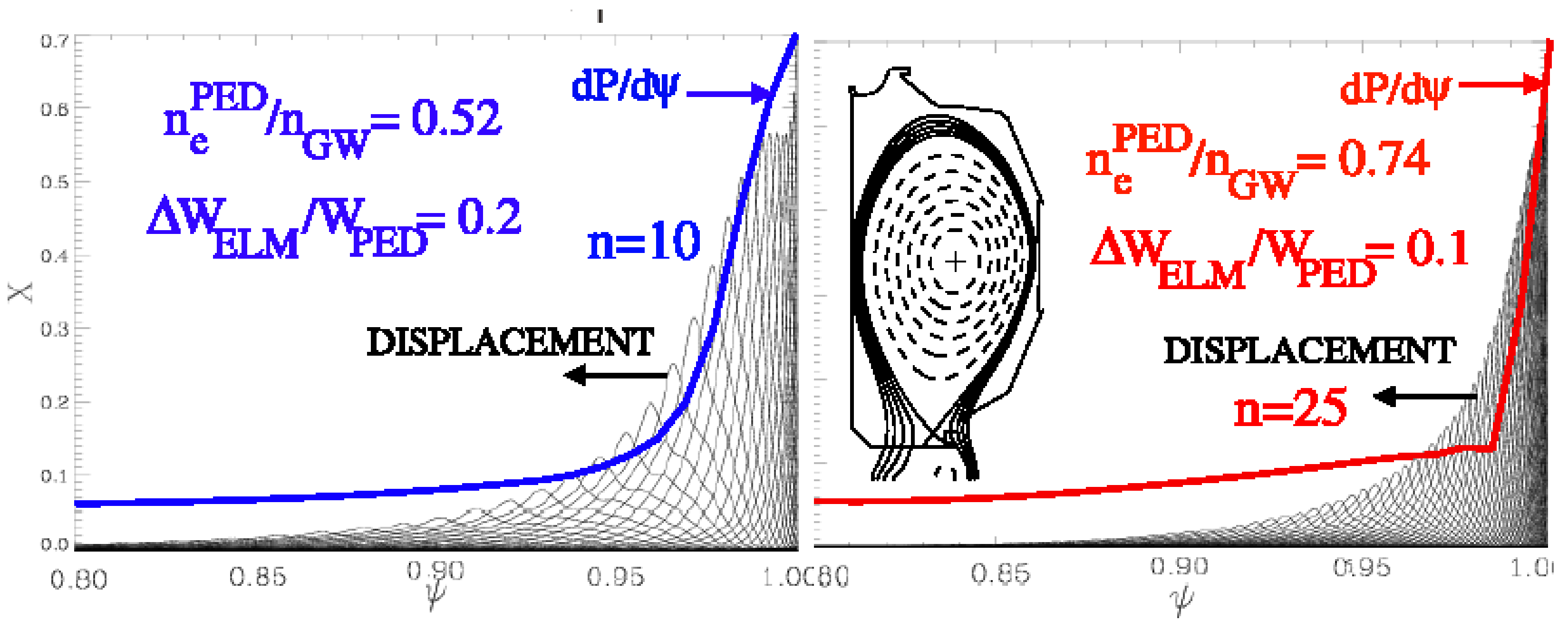

Linear Ideal MHD (GATO): Type I vs Type II ELMs

GATO (for AUG) S. Saarelma et al, NF(2003)

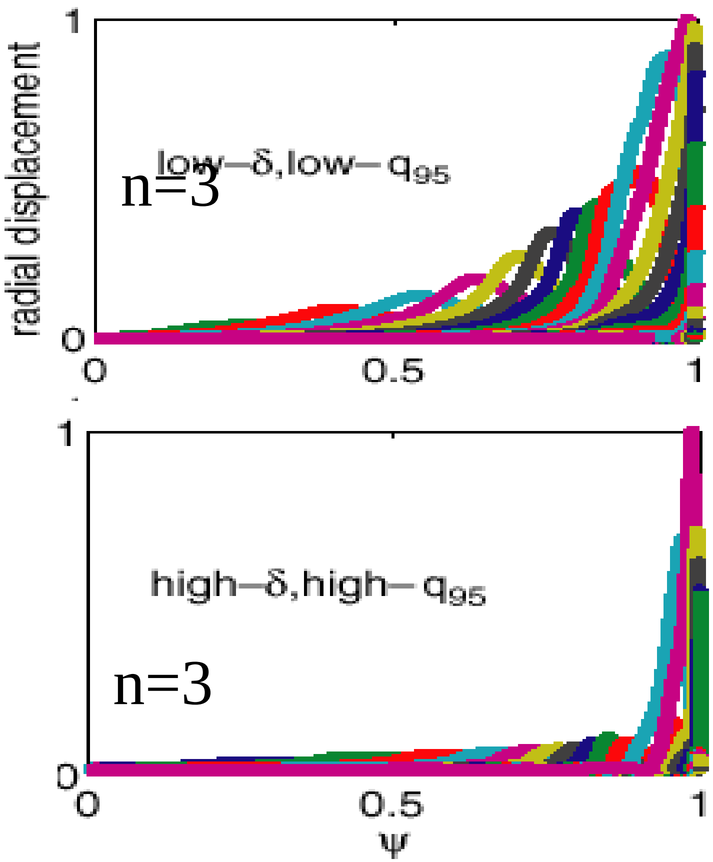

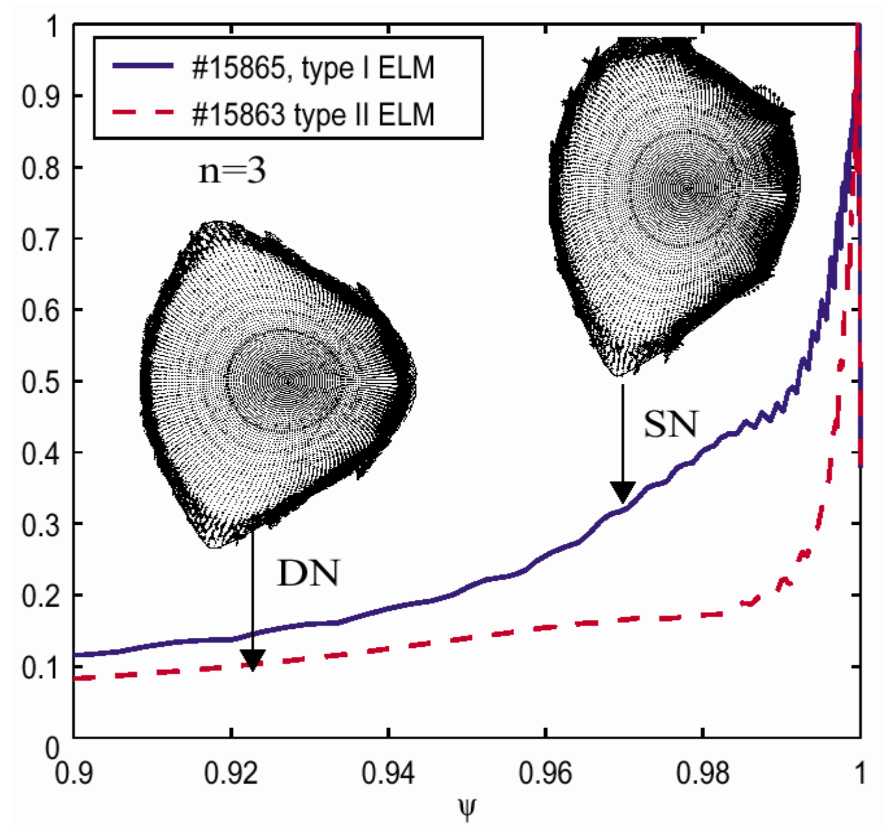

ELM affected area decreases at high q_{95} + high δ for the same pressure profile..

Radial Efflux from ELMs on MAST

TS profiles obtained near ELM peak show broad n_e tail on the outboard side

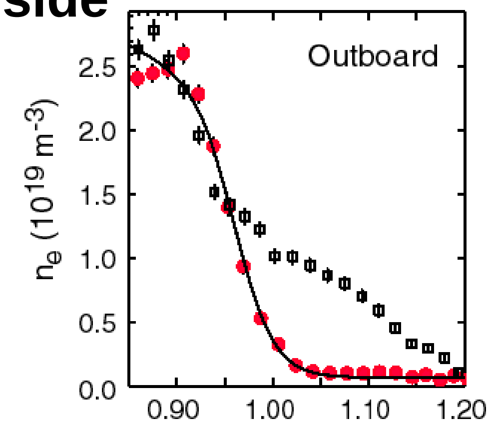

ELMs show D_a emission well beyond outboard separatrix

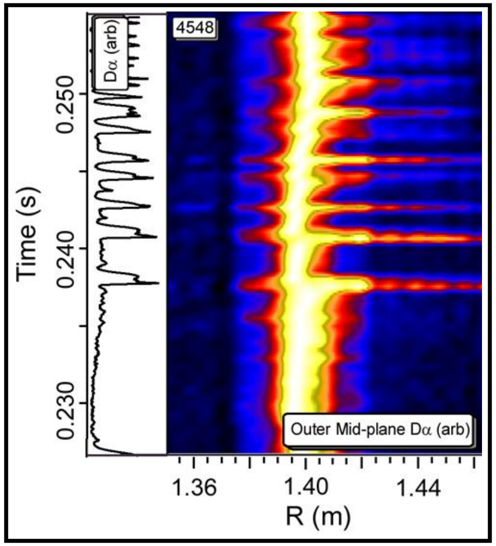

Large particle flux (J_{SAT}) to outboard mid-plane probe during ELM

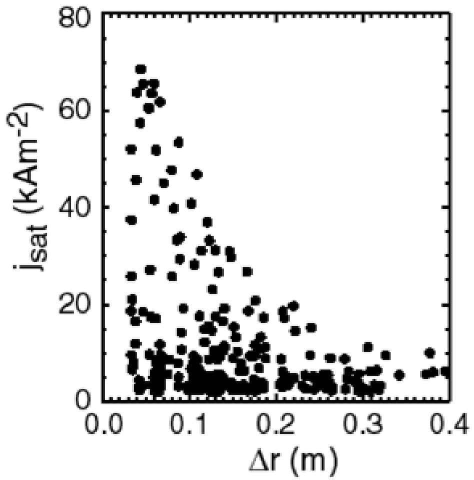

Radial efflux observed ~ 1 ELM in 5

The Non-linear Phase

ELM Spatial Structure

MAST

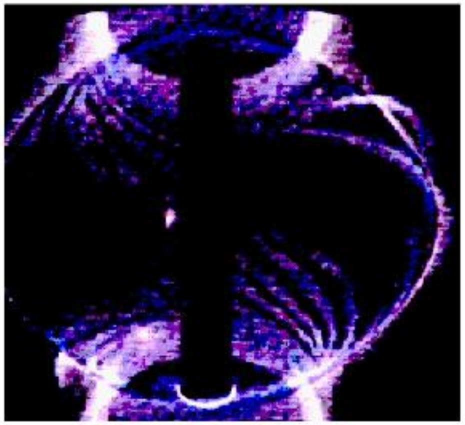

DIII-D

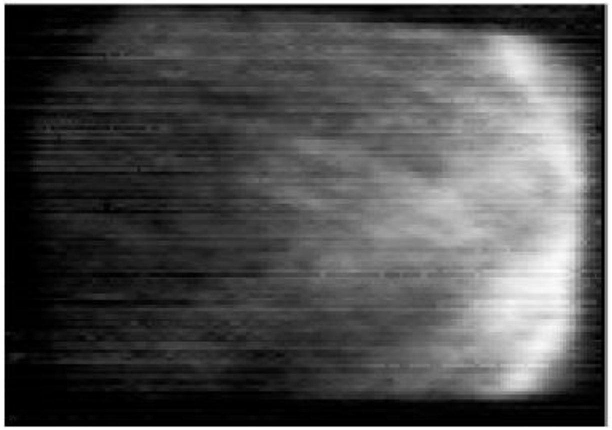

ASDEX Upgrade

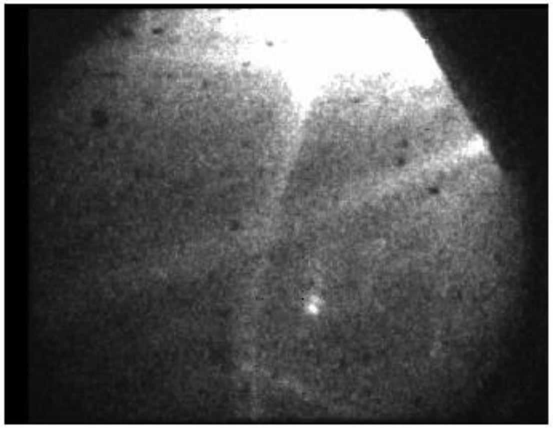

Filament structures clearly exist during ELMs
but what role do they play in the ELM loss mechanism ?

Filaments Characteristics

MAST

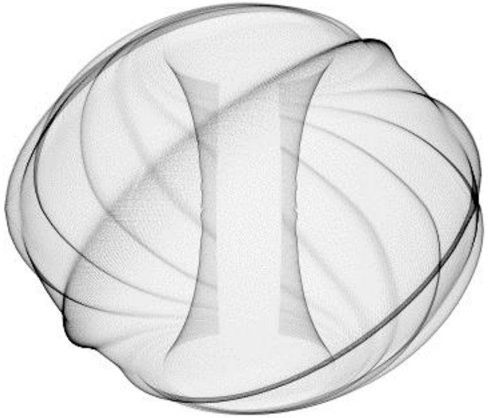

AUG

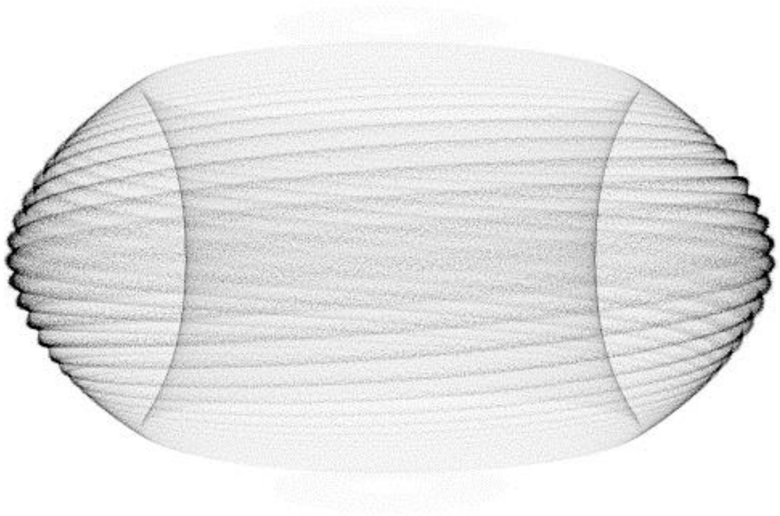

The structures appear to
- **follow the field lines**
- **have an extent perpendicular to the field line of ~ 5-10 cm**
- **toroidal mode number ~10-15**
- **radial velocities of 400 ms^{-1} (AUG) and 800 ms^{-1} (MAST)**
- **give radial effluxes up to 10 cm (AUG) and 20cm (MAST)**

Propagation of the Filaments

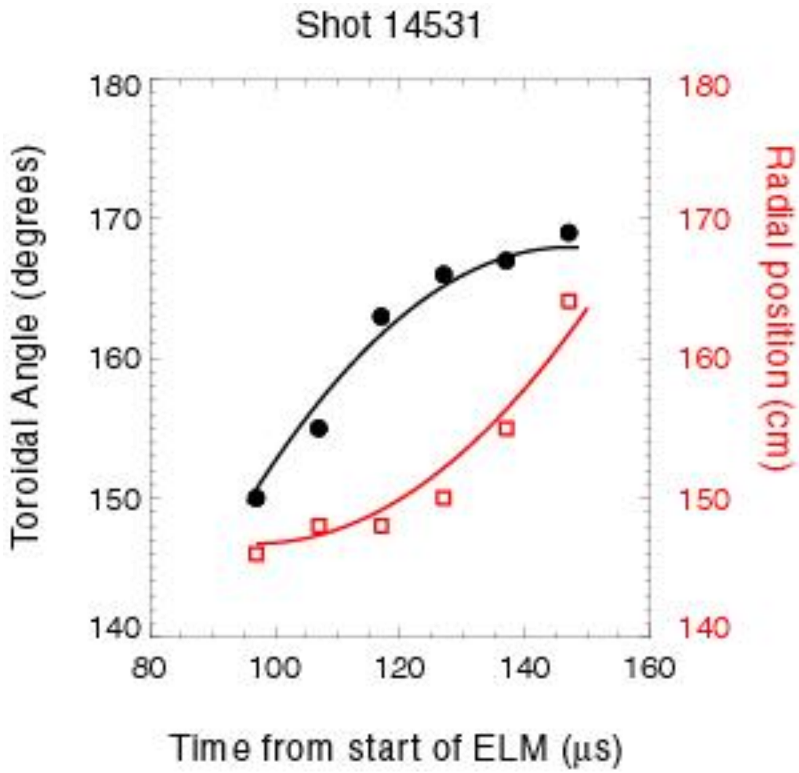

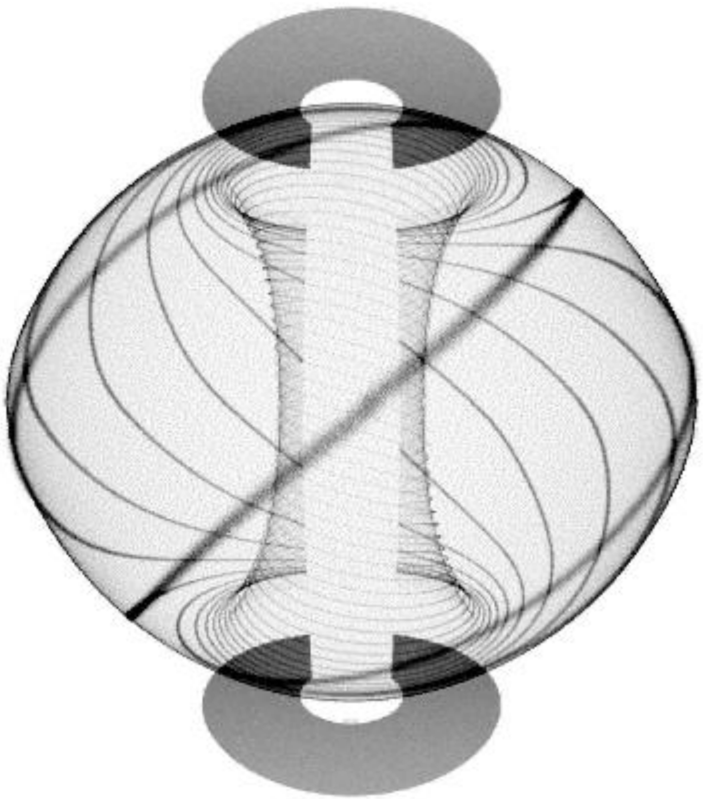

- **Decelerate toroidally**
- **Accelerate radially**

Propagation of the Filaments

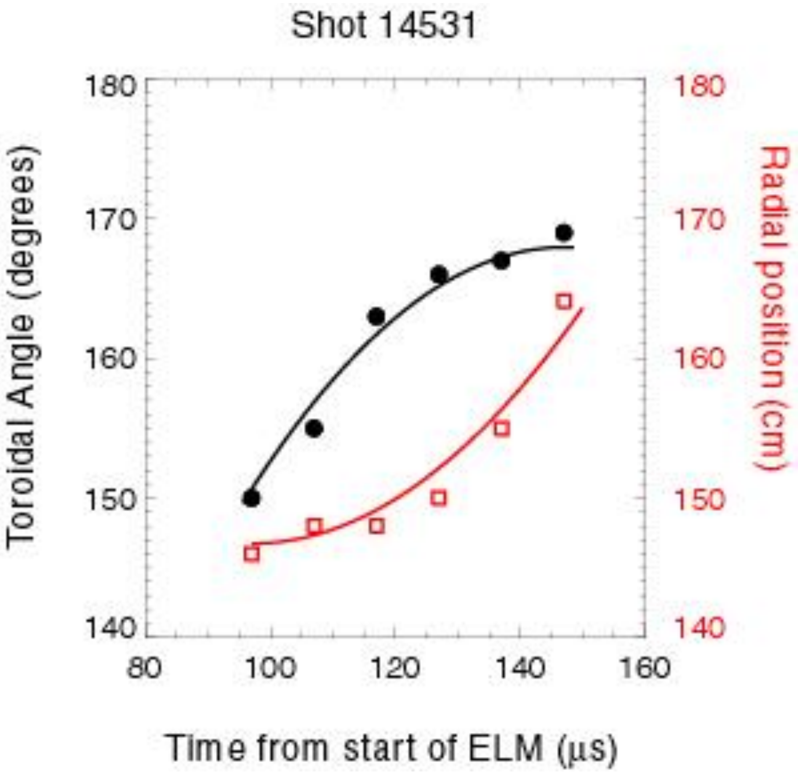

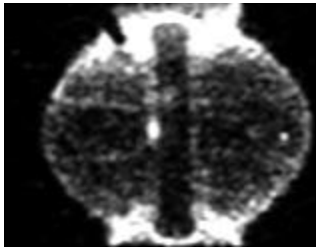

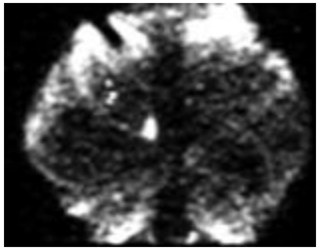

- **Decelerate toroidally**
- **Accelerate radially**

Radial Propagation of the Filaments

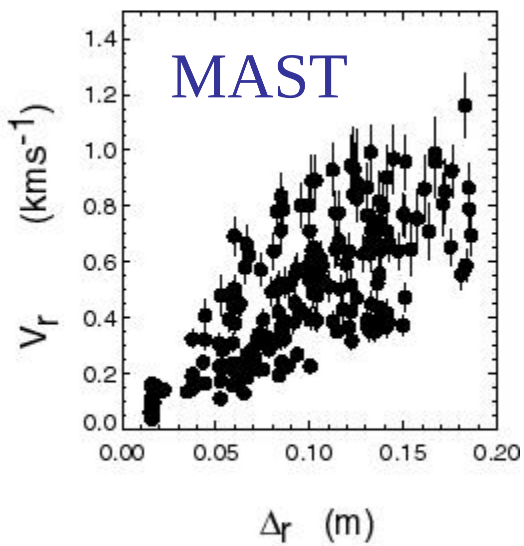

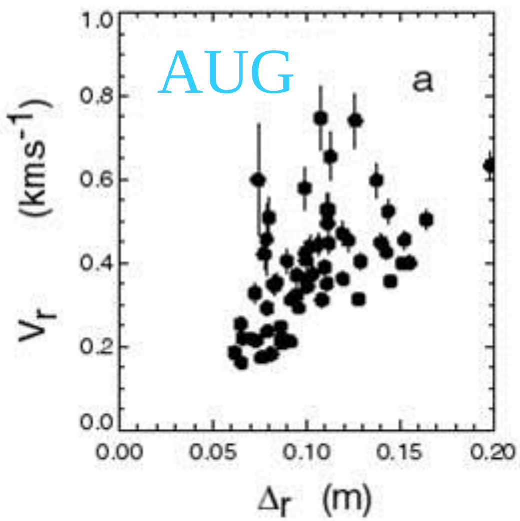

Accelerations ~ 5-15x10^6 ms^{-2}

Accelerations ~ 1.5-6.5x10^6 ms^{-2}

Analytic Theory

• **Non-linear models, and experimental data, indicate that the ballooning mode ejects a number (~10) filaments of hot plasma from the pedestal region**

•**Analytic theory for high-n modes (Cowley & Wilson):**

– **a tour de force of algebra, based on a number of approximations:**
  – **an ordering of spatial scales derived from linear theory**
  – **close proximity to marginal stability**
  – **periodicity boundary conditions assumed not to be important**

• **Predictions include:**

– **Ejected explosively from the pedestal**
– **The filaments are extended along field lines, but localised toroidally**
– **Hot filaments (flux tubes) of plasma are formed**

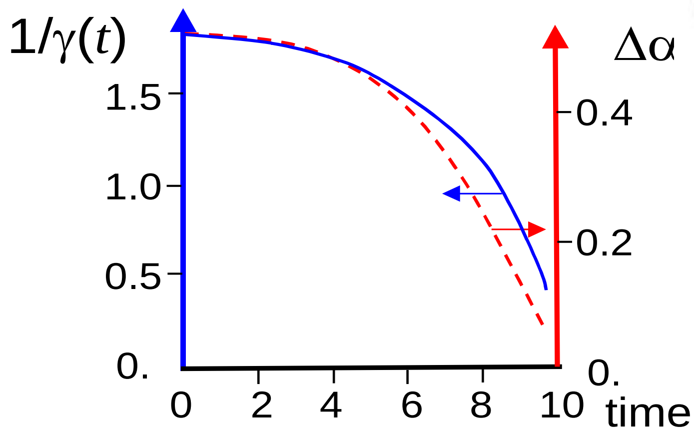

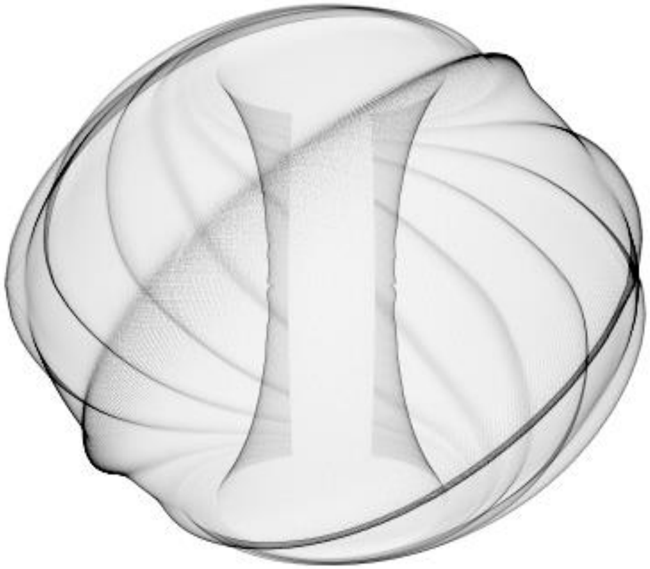

Numerical Studies of Non-linear Evolution

JOREK predicts low *n* modes appear to saturate

- **Numerical modelling of low-*n* kink modes:**
  - **Low *n* modes appear to saturate, rather than "explode"**
  - **Consistent with "outer" mode on JET and quasi-coherent mode of DIII-D**
  - **Could the existence of a saturated low *n* mode then suppress ELMs (eg as in QH-mode)?**

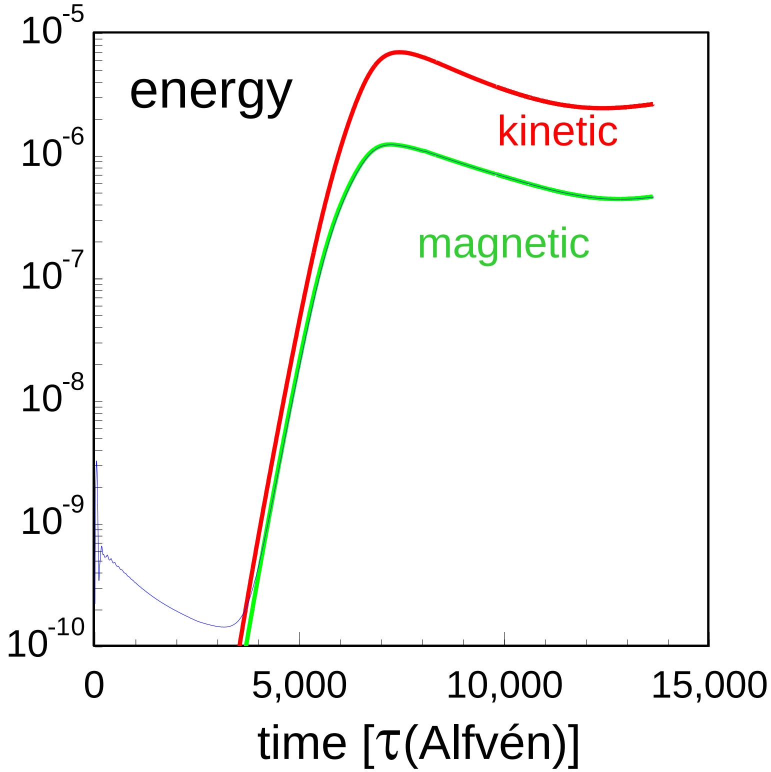

Huysmans, EPS 2005

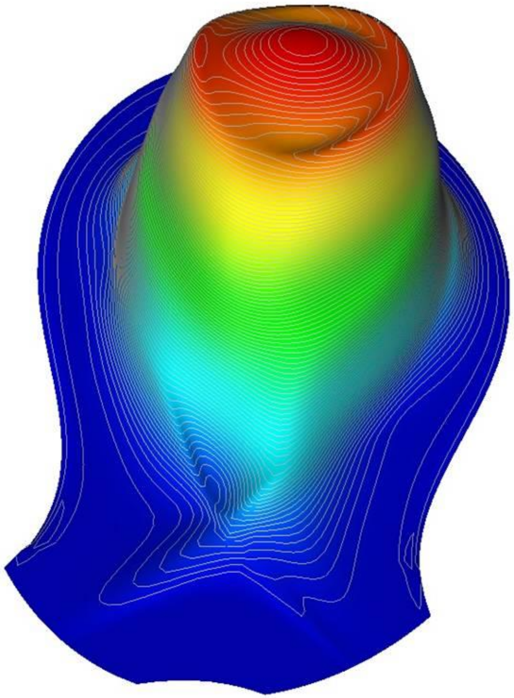

Density distribution

Numerical Studies of Non-linear Evolution

(S Jardin et al)

Nonlinear 2F ELM Computation with NIMROD

- Project's first large-scale 3D computation with Hall effect and Braginskii gyroviscosity.
- Nonlinear evolution from DIII-D 113317 equilibrium includes toroidal modes $0 \le n \le 42$.
- Linear two-fluid stabilization is obtained for large-n.
- Nonlinear coupling is producing poloidal localization, unlike our previous MHD results.

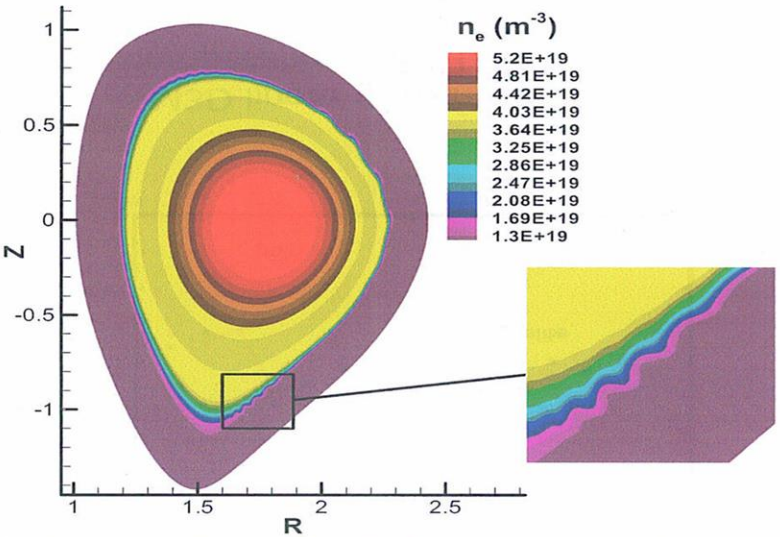

Number density in the ϕ=0 plane at simulation time t=82.3 μs has poloidally localized ripples.

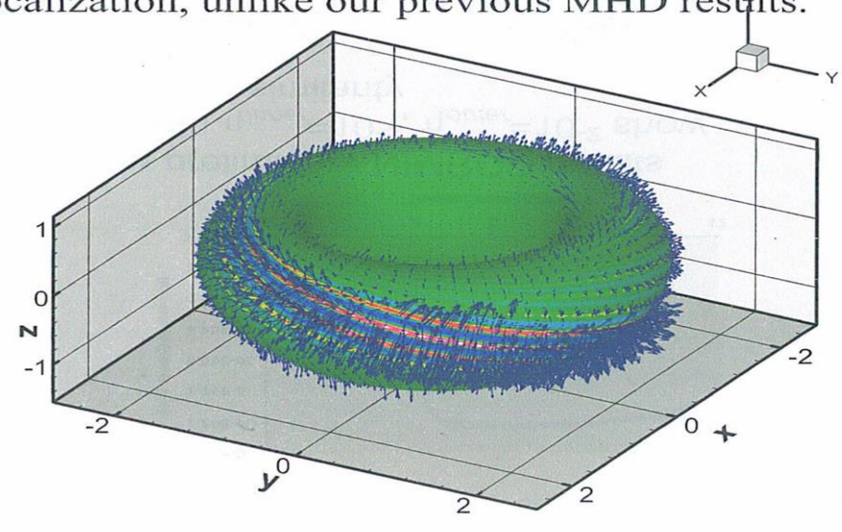

Temperature perturbations reach 100 eV at this time (T_{ped}=400 eV) and show a nonlinear helical structure. Perturbed plasma flow vectors are superposed.

Numerical Studies of Non-linear Evolution:
BOUT confirms explosive nature of intermediate *n* modes

- **Numerical modelling of intermediate-*n* modes:**
  - **Non-linear MHD codes being used to explore explosive behaviour**
  - **These use more advanced plasma models than the analytic theory, and are not subject to the same approximations**
  - **There are, of course, numerical limitations**
  - **BOUT does predict an instability with an explosive nature:**

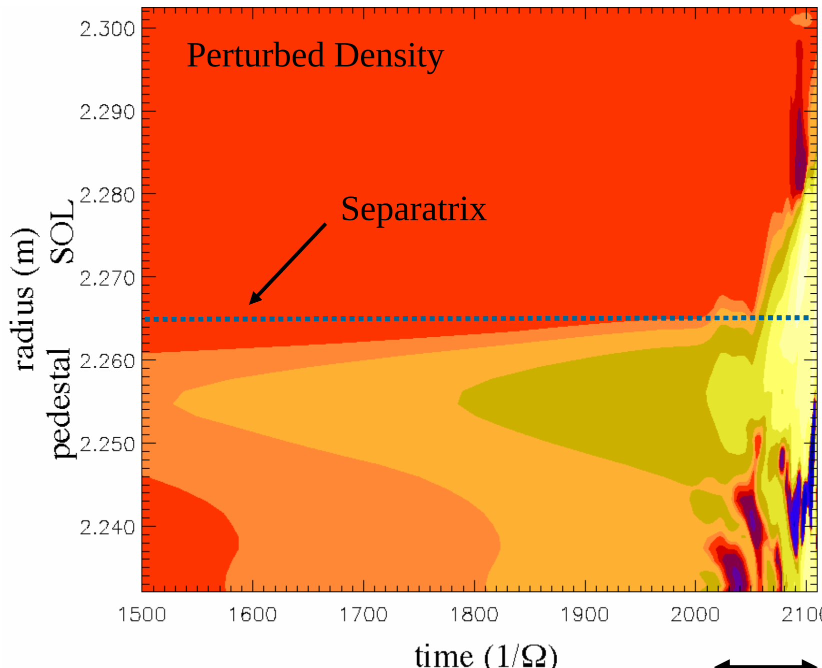

Mode grows in pedestal

Expels density into SOL: explosive

Surface of constant density perturbation

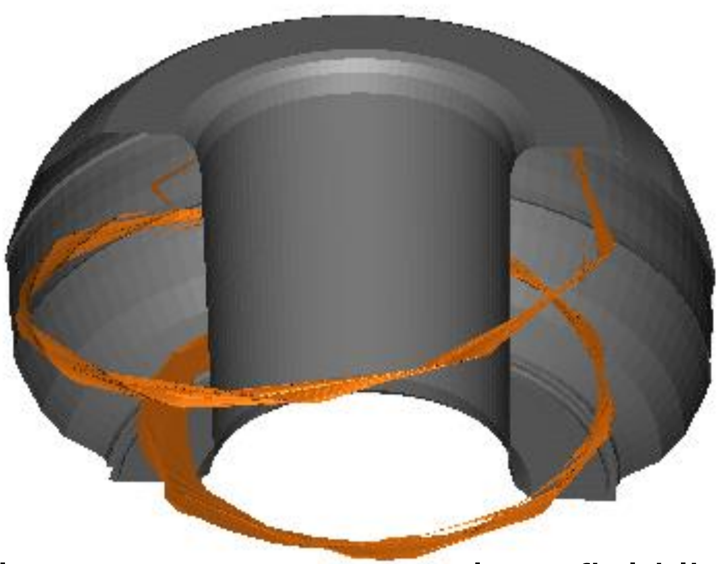

Filamentary structures along field lines

Snyder, EPS2005

The Post-crash State: Taylor Relaxation Theory

- Gimblett, Hastie and Helander have applied Taylor relaxation model to the pedestal region: by-passes details of the mechanism

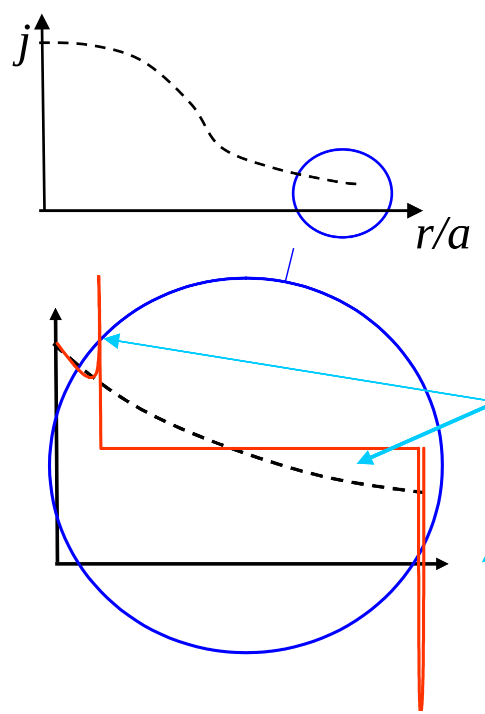

- Initial state is marginally peeling unstable
- Triggers the relaxation, minimising energy
  - conserve helicity
  - conserve poloidal flux in annulus
- Current flattens: destabilises peeling
- Skin currents form at boundaries of relaxed region
  - stabilising
- Peeling stability regained when width $\Delta > \Delta_c$
  - $\Rightarrow \Delta_c$ defines the ELM-affected region
- Predictions (MAST, high collisionality)
  - $\Delta W_{ELM}/W_{ped} \sim 1\%$
  - ELM width~few percent
  - large spread, depending on q_a

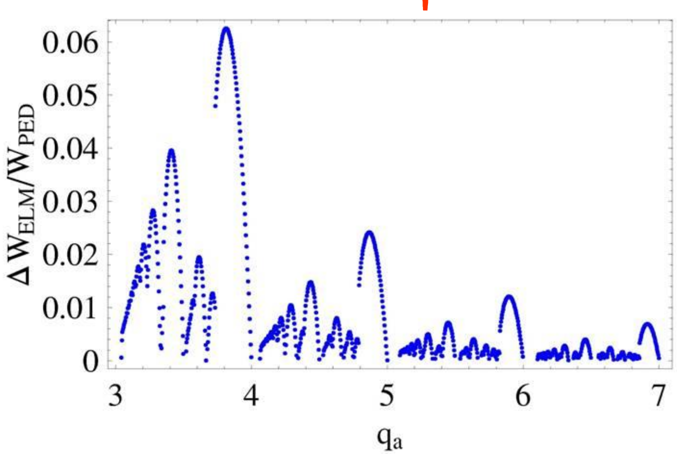

The ELM Cycle

- To address this question, a non-linear model is essential
- It must address:
  - The rapid, explosive growth of the ELM
  - Why the instability is transient and repetitive, rather than a steady, saturated mode
  - Or, better still, when is it a transient burst of activity and when is it steady, saturated mode?

Transport Code Modelling

- Evolve $\mathbf{j}, \mathbf{T_e}, \mathbf{n}$ with L-H mode transport
- Monitor trajectory in $j-\alpha$ stability diagram for trigger time
- Simulate losses δW_{ELM} by enhanced $\chi_\perp$ over Δr_{ELM} for time τ_{ELM}, say $\chi_\perp \sim 10\mathrm{m}^2\mathrm{s}^{-1}$ from turbulent transport
- Produces cyclical behaviour
- f_{ELM} given by reheating time

$\Longrightarrow$ need real physics-based models for $\chi_{\perp ELM}$, $\Delta r_{ELM}, \tau_{ELM}$ $\Longrightarrow$ non-linear model

Transport Code Modelling of ELM Cycle

ASTRA Simulations of the ELM Cycle

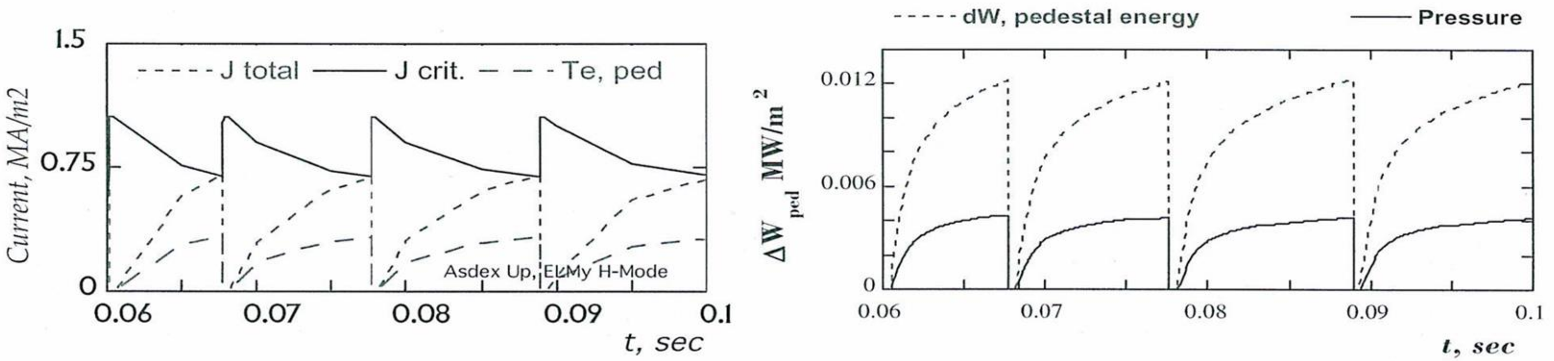

Fig. A Time evolution of the critical (blue) and total (red dashed) currents at the edge; pedestal electron temperature T_e (green)

Fig. B Time evolution of the stored pedestal energy ΔW_{ped} (red dashed) and total pressure (blue) at the edge;

UKAEA Fusion
Working with Europe

Physics Basis for ELM Cycle Modelling

- **Trigger – linear stability threshold**
- **Crash time** $\tau_{ELM} \sim \tau_{Alfven}\left(\tau_{Res}/\tau_{Alfven}\right)^{p}; p \sim 1/3 - 1$
- **Energy loss -** $\left(\dfrac{\delta W_{ELM}}{W}\right)_0 \sim \dfrac{\Delta_{ELM}}{a} \sim \dfrac{1}{nqs}$
- **But only really lost if ideal mode connects to divertor plate**

$$\Rightarrow \frac{\delta W_{ELM}}{W} \sim \left(\frac{\delta W_{ELM}}{W}\right)_0 \frac{1}{1+\tau_{\Box}/\tau_{ELM}} \qquad \tau_{\Box} = \pi Rq(1+\nu_{*e})/c_s$$

\- **fits data**

A Qualitative Analytic Model (Kerner, Pogutse et al)

- Ballooning mode in SOL
  - precursor expelling tube $\delta_1 \sim L_{px}$ in $\tau_1 \sim \sqrt{L_{px} R / C_s}$

$$\Rightarrow \frac{\delta W}{W} \sim \frac{L_p^2}{a^2} \frac{P_a}{< P >} \sim 10^{-3} : \text{ too small}$$

- Interacts with target plates, filling X-point with impurities
  - acts as effective limiter

  $\Rightarrow$ flute instability growing in $\tau_2 \sim \sqrt{L_{pa} R / C_s}$

- Produces Type I ELM, expelling $\Delta_{ELM} \sim a / nq$

- Refills on $\tau_3 \sim \tau_E (\Delta_{ELM} / a)^2$

- $\frac{\delta W_{ELM}}{W} \sim \frac{2}{nq} \frac{p_a}{< p >} \sim 5\% \text{ for n=1}$; $f_{ELM} \propto \frac{P}{\delta W} \propto \frac{BP}{I^3}$ - fits JET data!

Qualitative Mechanisms for Energy and Particle Loss in ELMs

- There are three possible contenders

  – The filaments act as 'leaky hosepipes': energy and particles diffuse from the hot filaments into the cold SOL: no reconnection required

  – The filaments act as a conduit, connecting the hot core plasma to the SOL target plates: reconnection is required

  – The filaments remove the sheared rotation in the plasma pedestal, which then collapses: no reconnection required

- These are just ideas: all need further work to place on a firm scientific basis

(1) The Leaky Hosepipe Model

- **Within the ideal MHD model, a hot flux tube of plasma twists and pushes out between field lines on neighbouring flux surfaces**
- **If no reconnection occurs, heat can only be lost through diffusion from the filament to the SOL**

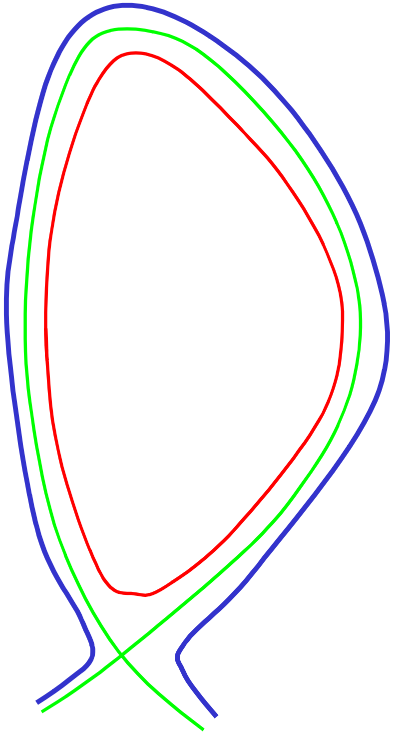

Pedestal becomes unstable to ballooning

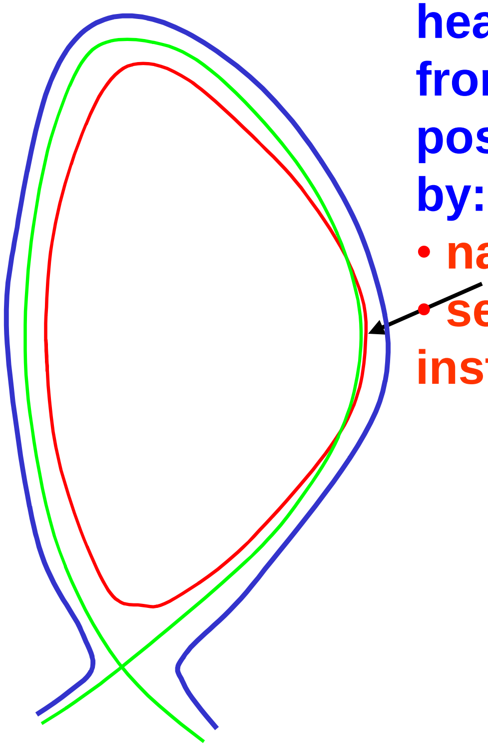

If no reconnection, heat/ptcles diffuse from filament to SOL, possibly enhanced by:

- **narrowing filaments**
- **secondary instabilities**

- **Theory predicts and expt observes filamentation**
- **Filament pushes out into SOL**

(2) Filament Reconnection: “Squirting Hosepipe”

- Reconnection would preferentially occur as the filaments cross the X-point
    - high magnetic shear would rip the filaments apart
- Flux tubes now connect hot pedestal directly onto SOL target plates
- Different mechanisms for DND and SND: DND ELMs more benign?

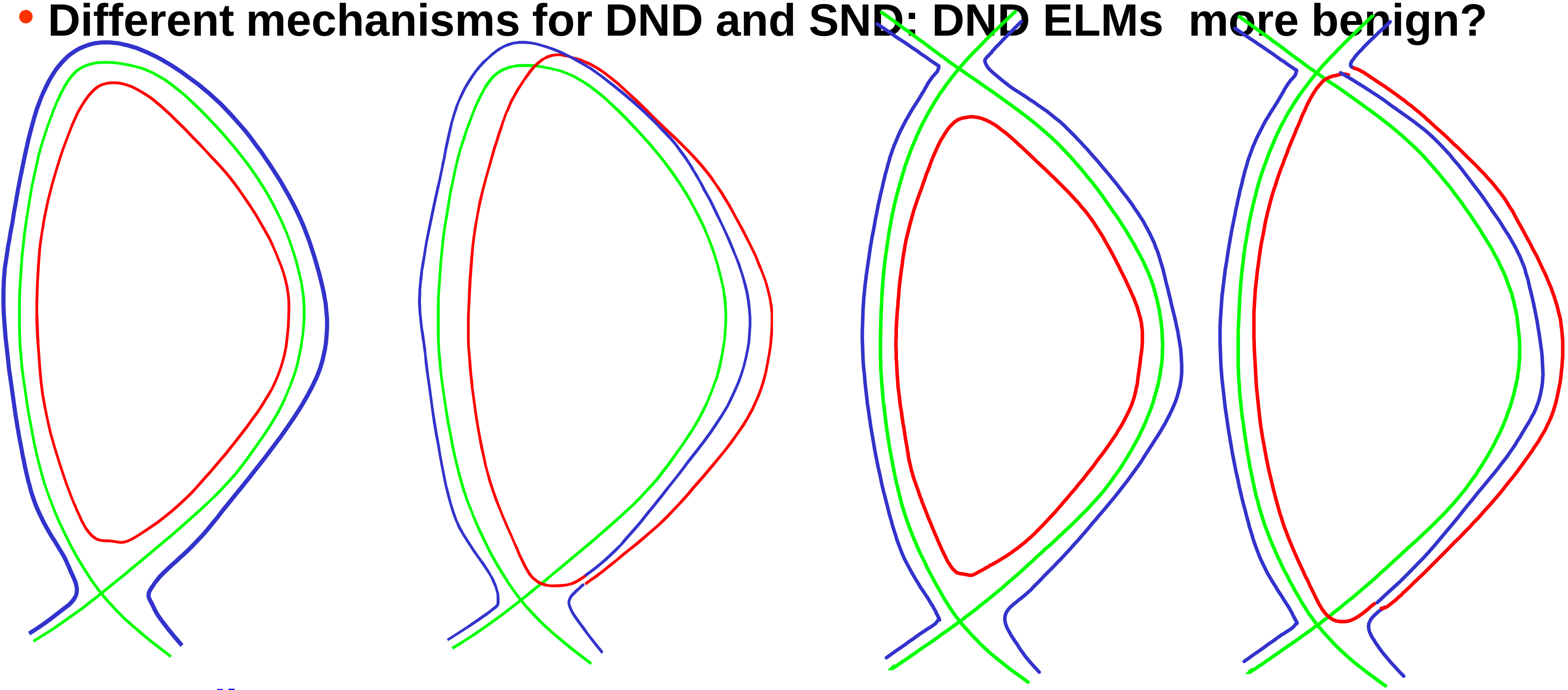

- SND: Filaments connect target plates via pedestal core plasma
- Heat/particles stream to target plates from pedestal

DND: Filaments break off:
Could repeat many times during an ELM?

(3) Flow Shear Suppression & Barrier Collapse

- Filaments can only be ejected if flow shear is suppressed
  - suppression of flow shear would lead to enhanced transport
  - barrier would collapse
- Flow shear is suppressed during an ELM, but :
  - does ballooning mode suppress flow shear leading to barrier collapse?
  - or does something else suppress flow shear, allowing ballooning modes to grow?

MAST

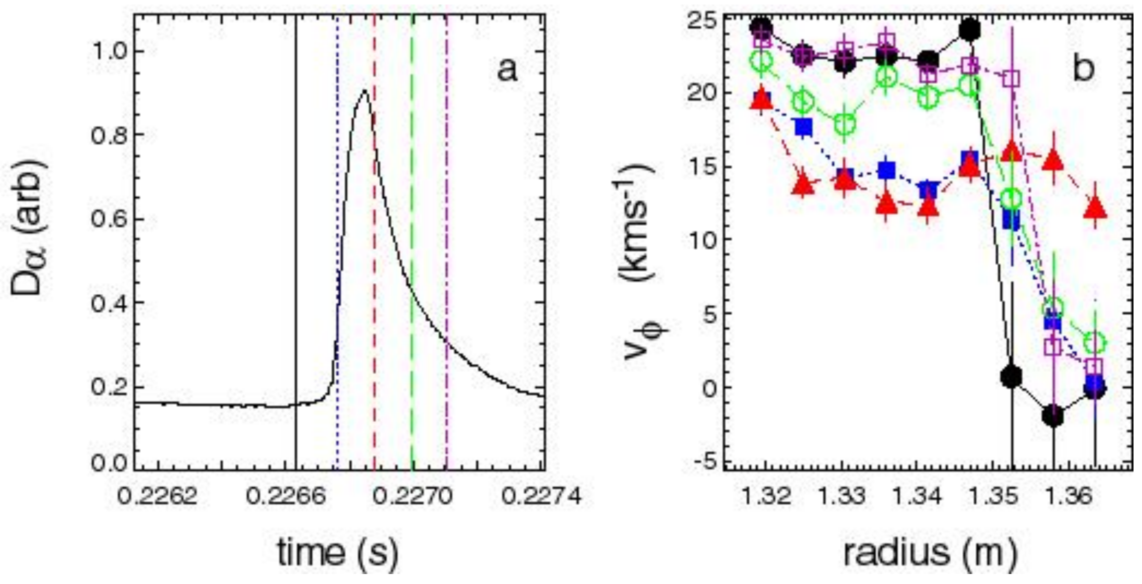

DIII-D

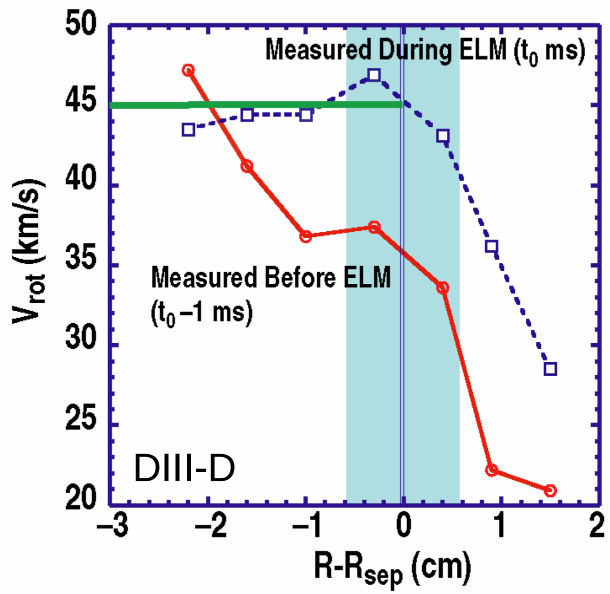

A Kirk, et al, PPCF 2005

Boedo, et al, Phys Plas 2005

Summary of Modelling

- We have the tools to study the non-linear evolutions, but they need more development

- Analytic theory provides simplified non-linear equations, but no final answer yet:
  - coefficients need to be determined
    - sign of quadratic non-linearity determines whether filament goes in or out
  - requires an efficient solution of non-linear equation for parameter scans
    - non-trivial due to finite time singularity and fractional derivatives
  - We are making progress here

- Numerical studies qualitatively confirm the analytic predictions for intermediate n, but more work is needed:
  - unable to produce the full ELM cycle from first-principles
  - what is the saturation mechanism?
  - what is the dominant transport mechanism?

ELM Control

Active ELM Control Techniques

- **ELM Control using magnetic coils**
- **ELM pacemaking using pellets**
- **Toroidal ripple**

ELM Control using Magnetic Coils

• **Stochastic Layer ELM Control on DIII-D**

• **Application of n=3 perturbation dramatically changes the character of the edge recycling.**

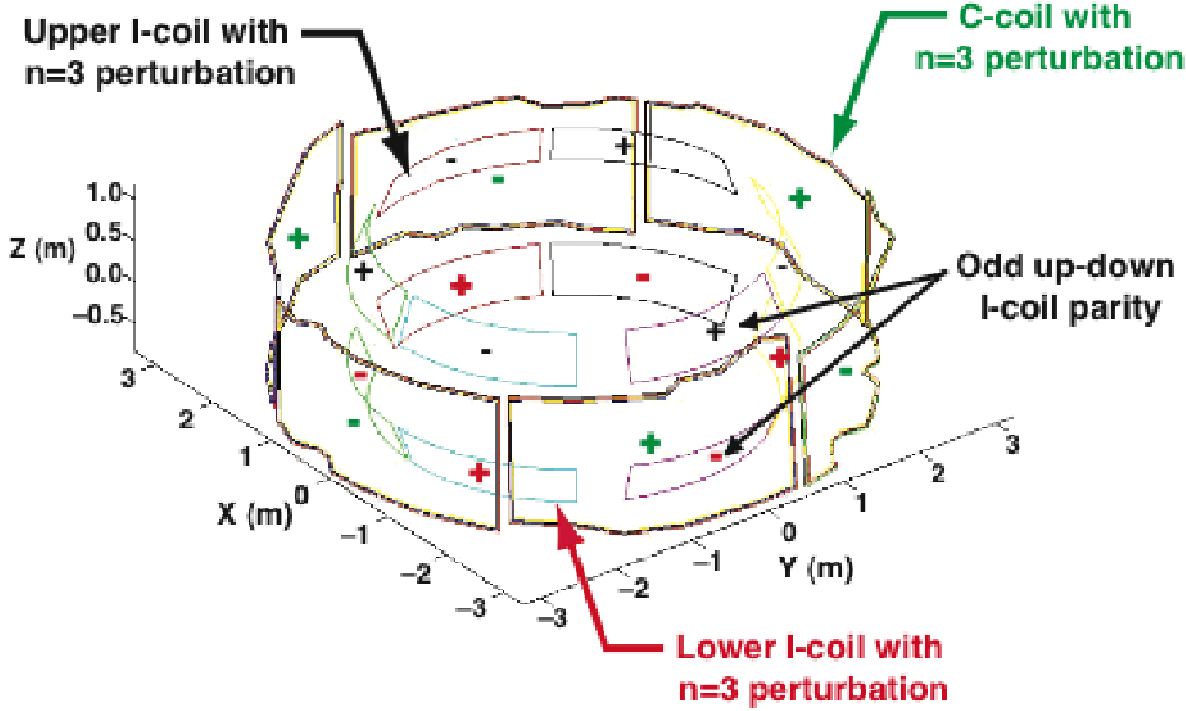

ELM Control using Magnetic Coils

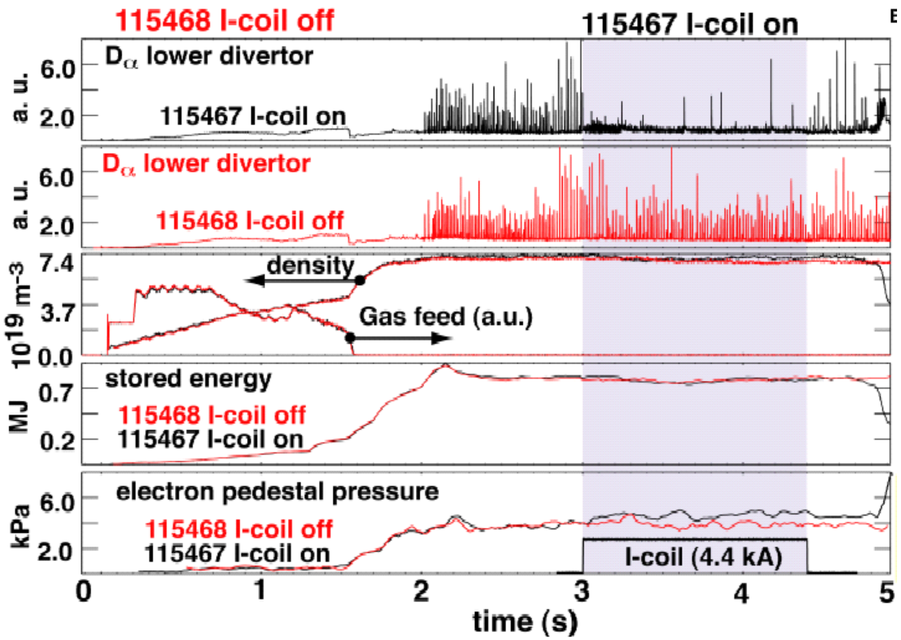

Dramatic reduction in ELM energy losses

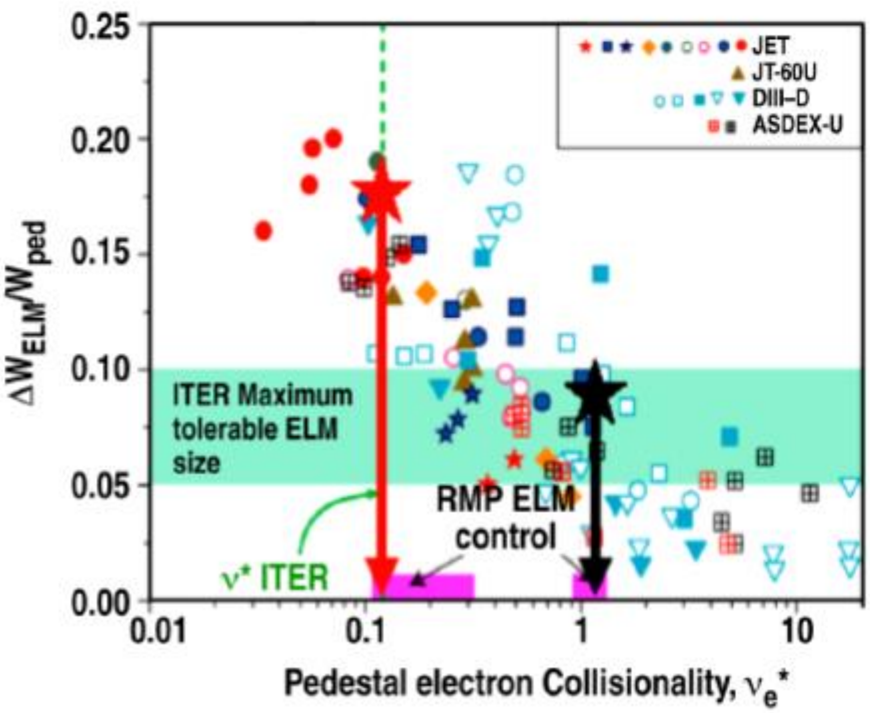

ELM Control using Pellet Pace Making

- **Pioneered on AUG**
- **ELMs are triggered by each pellet**

ASDEX Upgrade: pellet triggering

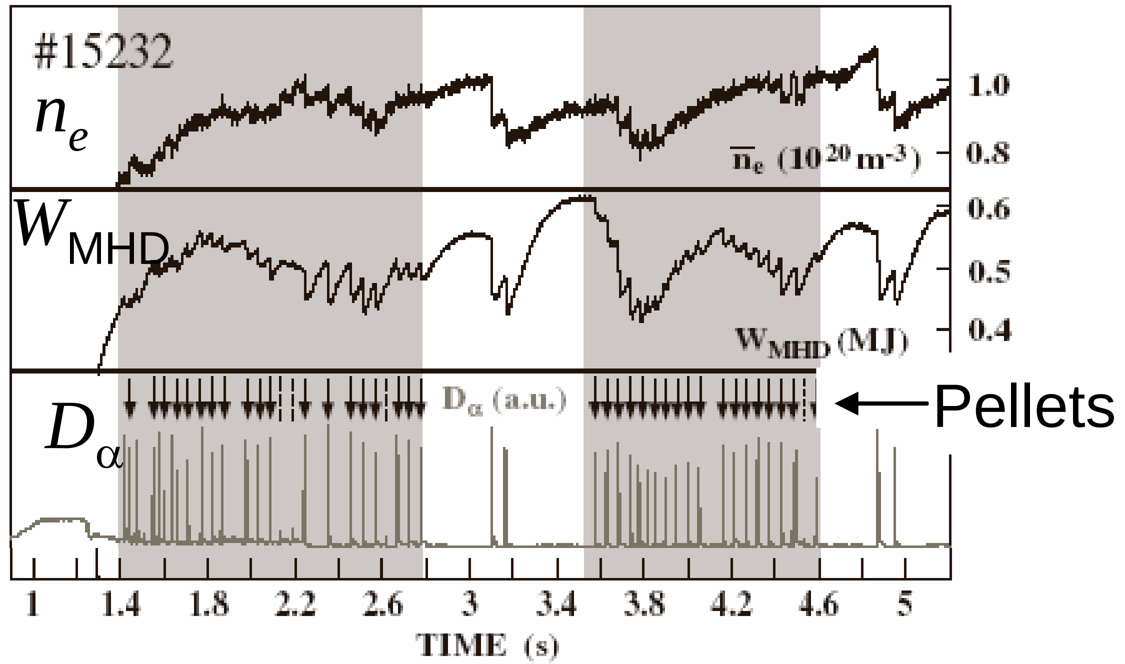

Effect of Toroidal Ripple

- In JT-60U the energy loss due to most of type I ELMs is less than ~6% of W_{ped}

- Thought to be due to the large toroidal ripple

- The downside is the poorer energy confinement time

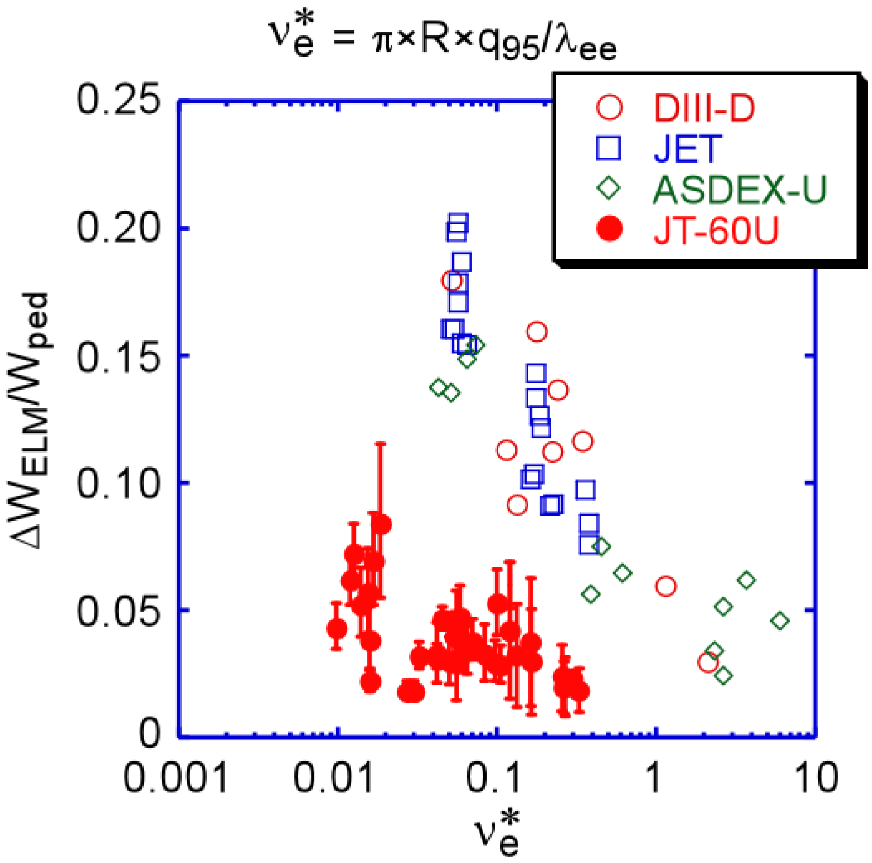

Stationary ELM-Free H-Mode

Regimes

Stationary ELM-Free H-Mode Regimes

- **EDA: Enhanced D-Alpha**
- **QH-mode: Quiescent H-mode**
- **HRS: High Recycling Steady H-mode**

EDA Mode

- **First seen on CMOD**
- **Observed at high density and low to modest heating power**
- **Observed at high edge collisionality $n_{95}/n_G > \sim 1.5$**
- **Global confinement can be as good as in Type I ELMy regimes**.

ALCATOR C-Mod

D Mossessian, PoP **10** (2003) 1720

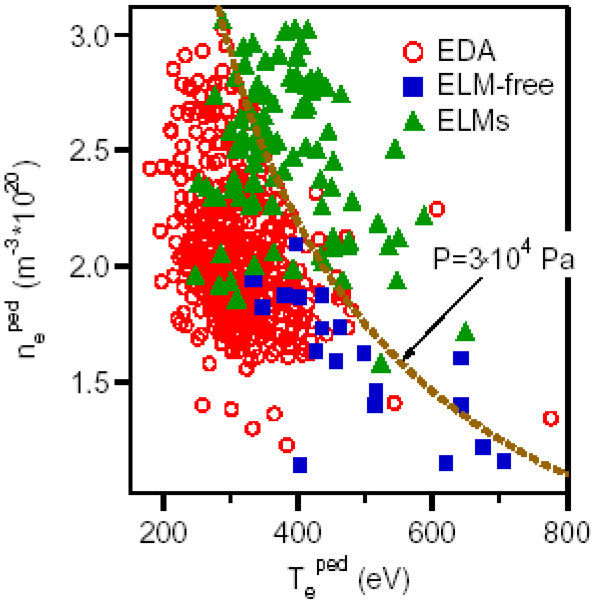

EDA Mode

• Density kept constant due to the existence of a quasicoherent (QC) mode (50-120 Khz range high n,m)

• In similarity experiments AUG and DIII-D have seen a QC but have not established a steady state regime

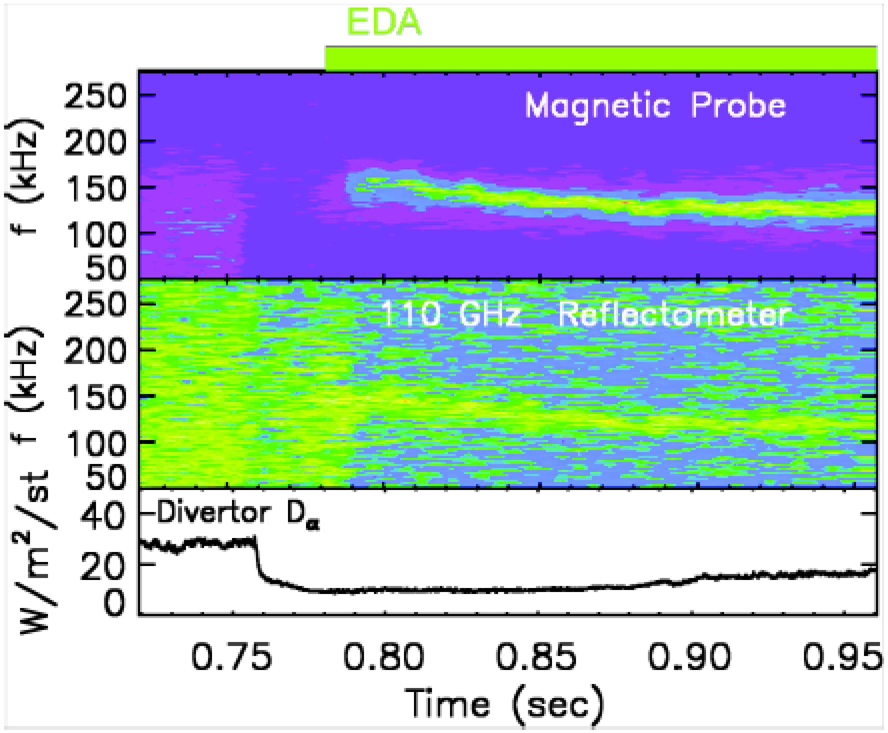

Q-H Mode

- First seen on DIII-D – robustly reproduced on AUG
- Only observed in counter NBI with a large plasma wall distance (suggesting a role of fast ions)
- Low density regime ($n_e/n_G \sim 0.04$) pedestal pressures comparable to Type I ELMy H-mode

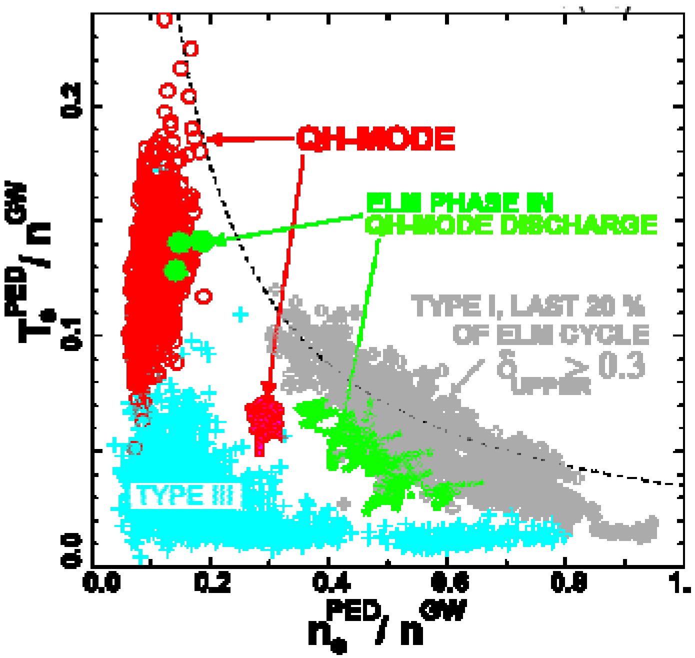

Q-H Mode

- **Edge Harmonic Oscillation typically observed, non sinusoidal mode giving a mix of toroidal mode numbers (n=1,2,3,4,…, f(n=1) 5-11 kHz). Possibly accompanied by a HFO (350-500 kHz)**

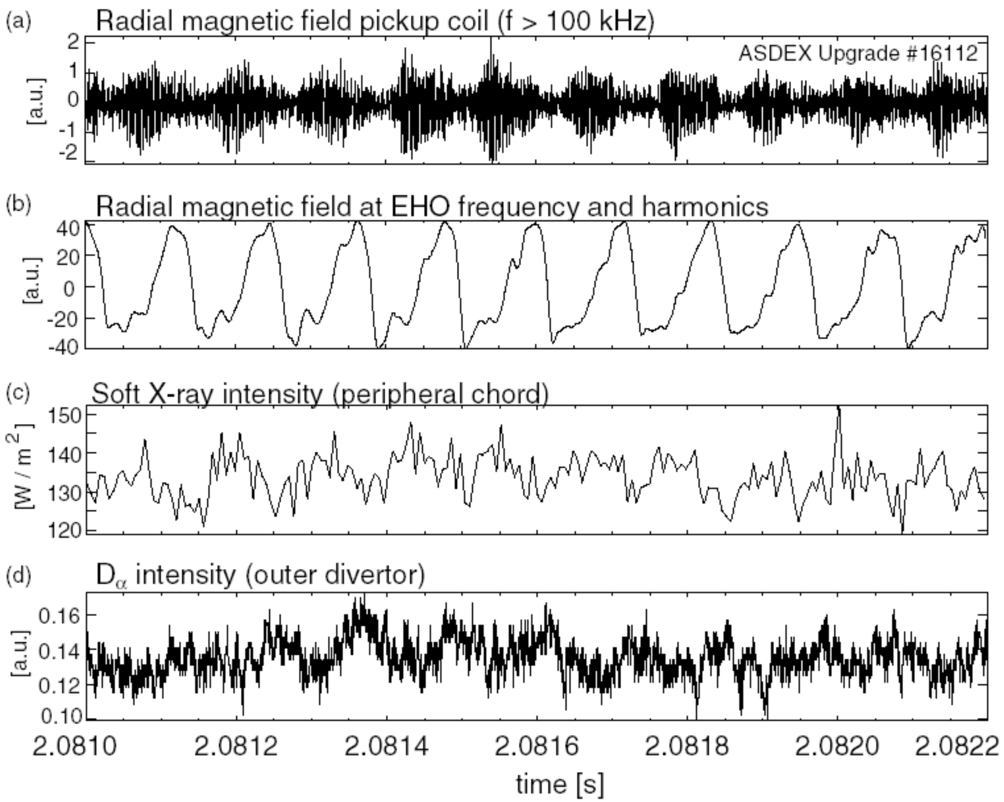

HRS Mode

- **First seen on JFT-2M**
- **Very similar to EDA**
- **Access favours high density and neutral pressure.**
- **High edge collisionality**
- **High frequency (>100 kHz) edge modes observed.**

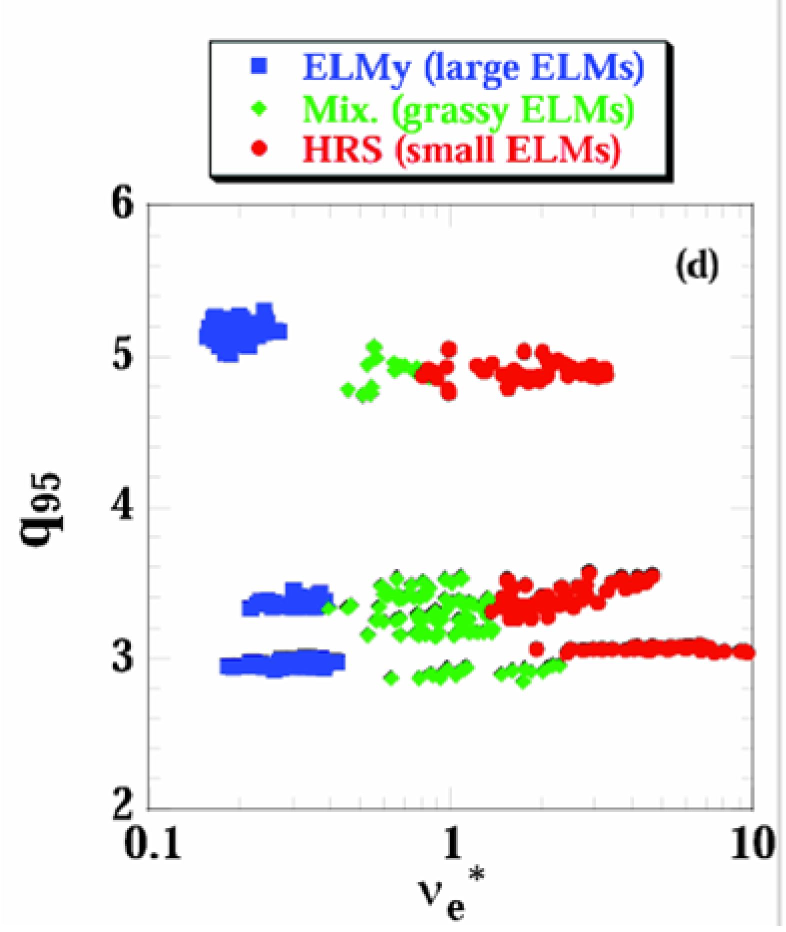

Summary: What we believe we know

- Type I ELMs are triggered by ideal MHD peeling-ballooning modes

- Most ELMs seem to be associated with filamentary structures

- Flow shear is suppressed during an ELM

Summary: What we think we know

- **The plasma current density plays an important role**
  - **high plasma current density results in large ELMs**

- **Toroidal flows need to approach sonic speeds to have an impact on ELM trigger: what about the impact on the non-linear evolution?**

- **Diamagnetic effects are important at the edge, reducing growth rates**
  - **plasmas with strong diamagnetic effects may have smaller ELMs (high β_θ, q)**

- **There seems to be a correlation between ELM size and linear eigenmode width**
  - **ELM affected area not always determined by eigenmode, but sometimes is**

- **Ergodising magnetic field in pedestal can hold gradients below stability threshold: suppresses ELMs**

Summary: What we don't know

- The implications of separatrix geometry is not clear
  - is the ideal MHD peeling mode stabilised? Seems to be
  - a resistive peeling mode is predicted
  - what is the impact of open field lines of the SOL?
- Is current ejected during the ELM: what mechanism, and how fast?
- While filaments are associated with ELMs, are they a cause or an effect?
- If the cause, how do they lead to heat loss?
  - suppression of shear flow in barrier?
  - act as a tube, connecting pedestal to SOL?
  - is reconnection important?
- In the no-ELM regimes (QH and EDA mode), what suppresses ELMs?
- What is the mechanism behind the pellet-triggered ELMs?
  - Why are they smaller?
- What is the key ingredient to achieve small ELMs?

Final Summary

- **Many different ELMing and ELM free regimes exist – most are not ITER relevant – but do increase our understanding**

- **The Type I ELM regime is the basis for ITER operation – there are potential ways to decrease their impact onto plasma facing components**

- **The more we can understand about the ELM the easier it is to make quantitative predictions for future devices**

- **A predictive ELM model is critically needed**